INHIBITION OF CELL PROLIFERATION THROUGH REGULATED

INTRAMEMBRANE PROTEOLYSIS OF CREB3L1

APPROVED BY SUPERVISORY COMMITTEE

Jin Ye, Ph.D.

Supervising Professor

Julie Pfeiffer, Ph.D.

Chair, Examining Committee

Nicholas Conrad, Ph.D.

Committee Member

Ivan D'Orso, Ph.D.

Committee Member

This thesis is dedicated to my parents and my wife:

My parents for always stressing the importance of higher education.

My wife for being a constant source of encouragement and for supporting my endeavors.

Especially the crazy ones.

INHIBITION OF CELL PROLIFERATION THROUGH REGULATED INTRAMEMBRANE PROTEOLYSIS OF CREB3L1

by

Bray Standard Denard

DISSERTATION

Presented to the Faculty of the Graduate School of Biomedical Sciences

The University of Texas Southwestern Medical Center at Dallas

In Partial Fulfillment of the Requirements

For the Degree of

DOCTOR OF PHILOSOPHY

The University of Texas Southwestern Medical Center at Dallas

Dallas, Texas

March, 2012

Acknowledgements

I would like to thank Dr. Jin Ye for meticulously mentoring me to become a top notch scientist. Under Jin's intruction, I've learned how to tackle scientific problems in a clear and unbiased manner. I also thank Dr. Hua Huang as his work laid the foundation for my success as a graduate student.

I would like to acknowledge the people of the tissue culture core for making experiments very easy to perform in an efficient manner. Especially Lisa Betty for her tireless work in tissue culture that allows us to quickly generate the tools we need to further our research.

I give my gratitude to Saada Abdalla, Jeff Cormier, Angela Carroll, Nancy Heard, Dr. Y.K. Ho, and Linda Donelly for their technical assistance. Research would be very difficult without the wonderful support they provide.

I thank current and past committee members Dr. Julie Pfeiffer, Dr. Nicholas Conrad, Dr. Pinghui Feng, and Dr. Ivan D'Orso for their advice and time. I especially thank Dr. Ivan D'Orso, who took Dr. Feng's place on very short notice.

I am grateful to Drs. Brown and Goldstein for building a department that places a deep emphasis on quality research. Their constructive criticism and insights have allowed me to fully explore the scope of my research and carry it to the next level.

Finally, I deeply appreciate the support and encouragement I've received from my friends and family. I thank my parents for encouraging me to seek higher education. I thank my wife for wonderfully supporting me through failure and success.

INHIBITION OF CELL PROLIFERATION THROUGH REGULATED INTRAMEMBRANE PROTEOLYSIS OF CREB3L1

Bray Standard Denard, Ph.D.

The University of Texas Southwestern Medical Center at Dallas, 2012

Mentor: Jin Ye, Ph.D.

CREB3L1/OASIS is a cellular transcription factor synthesized as a membrane-bound precursor and activated by regulated intramembrane proteolysis in response to stimuli like ER stress. By comparing gene expression between Huh7 subclones that are permissive for hepatitis C virus (HCV) replication versus the non-permissive parental Huh7 cells, we identified CREB3L1 as a host factor that inhibits proliferation of virus-infected cells. Upon infection with diverse DNA and RNA viruses, including murine γ-herpesvirus 68, HCV, West Nile virus (WNV), and Sendai virus, CREB3L1 was proteolytically cleaved, allowing its NH2 terminus to enter the nucleus and induce multiple genes encoding inhibitors of the cell cycle to block cell proliferation. Consistent

with this, we observed a necessity for CREB3L1 expression to be silenced in proliferating cells that harbor replicons of HCV or WNV. Our results indicate that CREB3L1 may play an important role in limiting virus spread by inhibiting proliferation of virus-infected cells.

Doxorubicin is used extensively for chemotherapy of diverse types of cancer, yet the mechanism through which it inhibits proliferation of cancer cells remains unclear. Here we report that doxorubicin stimulates *de novo* synthesis of ceramide, which in turn activates CREB3L1, a transcription factor synthesized as a membrane-bound precursor. Doxorubicin stimulates proteolytic cleavage of CREB3L1 by Site-1 Protease and Site-2 Protease, allowing the NH_2-terminal domain of CREB3L1 to enter the nucleus where it activates transcription of genes encoding inhibitors of the cell cycle, including *p21*. Knockdown of CREB3L1 mRNA in human hepatoma Huh7 cells and immortalized human fibroblast SV589 cells conferred increased resistance to doxorubicin, whereas overexpression of CREB3L1 in human breast cancer MCF-7 cells markedly enhanced the sensitivity of these cells to doxorubicin. These results suggest that measurement of CREB3L1 expression may be a useful biomarker in identifying cancer cells sensitive to doxorubicin.

Table of Contents

Prior Publications

Denard, B. and Ye, J. (2012). Doxorubicin blocks proliferation of cancer cells through proteolytic activation of CREB3L1. Submitted

Denard, B., Seemann, J., Chen, Q., Gay, A., Huang, H., Chen, Y., and Ye, J. (2011). The membrane-bound transcription factor CREB3L1 is activated in response to virus infection to inhibit proliferation of virus-infected cells. Cell Host Microbe *10*, 65-74.

Wu, Z., Luby-Phelps, K., Bugde, A., Molyneux, L.A., Denard, B., Li, W.H., Suel, G.M., and Garbers, D.L. (2009). Capacity for stochastic self-renewal and differentiation in mammalian spermatogonial stem cells. J Cell Biol *187*, 513-524.

Hao, J., Yamamoto, M., Richardson, T.E., Chapman, K.M., Denard, B.S., Hammer, R.E., Zhao, G.Q., and Hamra, F.K. (2008). Sohlh2 knockout mice are male-sterile because of degeneration of differentiating type A spermatogonia. Stem Cells *26*, 1587-1597.

Dann, C.T., Alvarado, A.L., Molyneux, L.A., Denard, B.S., Garbers, D.L., and Porteus, M.H. (2008). Spermatogonial stem cell self-renewal requires OCT4, a factor down-regulated during retinoic acid-induced differentiation. Stem Cells *26*, 2928-2937.

McCormick, C.C., Hobden, J.A., Balzli, C.L., Reed, J.M., Caballero, A.R., Denard, B.S., Tang, A., and O'Callaghan, R.J. (2007). Surfactant protein D in Pseudomonas aeruginosa keratitis. Ocul Immunol Inflamm *15*, 371-379.

List of Appendices

List of Abbreviations

ATF6, Activation Transcription Factor 6

BMP2, Bone Morphogenetic Protein 2

CHO, Chinese Hamster Ovary

CREB3L1, Cyclic AMP Response Element 3 Like 1

CMV, Cytomegalovirus

E1, E2, Envelope glycoprotein 1 and 2

ER, Endoplasmic Reticulum

GFP, Green Fluorescent Protein

HCV, Hepatitis C Virus

HPV, Human Papilloma Virus

HSV, Herpes Simplex Virus

HRP1, HCV Replication-Permissive 1

IRES, Internal Ribosomal Entry Site

NS2, NS3, NS4A-B, NS5A-B, Non-Structural Protein 2, 3, 4A-B, 5A-B

OASIS, Old-Astrocyte Specifically Induced Substance

PDI, Protein Disulfide Isomerase

ROS, Reactive Oxygen Species

RIP, Regulated Intramembrane Proteolysis

RT-QPCR, Real Time-Quantitative Polymerase Chain Reaction

S1P, Site-1 Protease

S2P, Site-2 Protease

SREBP, Sterol Regulatory Element Binding Protein

TK, Thimidine Kinase

UTR, Untranslated Region

WNV, West Nile Virus

Chapter 1: Introduction

Hepatitis C Virus Background

Hepatitis C Virus (HCV) is a blood borne pathogen that infects 170-180 million people worldwide. In most patients, HCV infection leads to chronic infection. Chronically infected patients may develop cirrhosis and/or hepatocellular carcinoma. Due to these complications, HCV infected patients are the major recipients of liver transplant in the United States and Europe (Appel et al., 2006; Ye, 2007).

HCV is a member of genus *Hepacivirus* and family *Flaviviridae*. HCV is a positive sense, single stranded RNA virus with a 9.6 kilobase viral genome. HCV has a single open reading frame that is translated via an upstream Internal Ribosomal Entry Site (IRES) site into a single polyprotein which is then processed into the 10 major HCV proteins by a combination of host peptidases and viral proteases (Fig. 1). Core, E1, E2, and p7 proteins are cleaved from the polyprotein by cellular signal peptidases. NS2 auto-cleaves itself from NS3, then NS3 and NS4A form a serine protease complex that cleaves NS4B, NS5A, and NS5B proteins. Core, E1, and E2 are categorized as structure proteins due to the fact that they are the proteins that eventually form the viral capsid. The remaining proteins are categorized as non-structural proteins and are involved in replication and assembly of the virus (Appel et al., 2006; Moradpour et al., 2007).

Current therapy of HCV consists of pegylated interferon with ribavarin or protease inhibitors, Telapravir and Bocepravir. While this therapy is effective in 50-80% of cases, it has very serious side effects that some patients cannot tolerate. Additionally, these treatments are extremely expensive (Aman et al., 2012). Owing to the error prone

replication of HCV's RNA genome, HCV can quickly generate mutant viruses that do not respond to therapy. In fact, many HCV mutations have been reported that render these treatments ineffective (Thompson et al., 2011; Yuan et al., 2010). While most therapies target viral factors (Rice, 2011), very few therapies are designed to activate host immune response. Targeting the activation of host immune response would have several advantages over targeting viral proteins. The major advantage is that host proteins do not evolve and the rapid rate of viral proteins, thus avoiding the problem of viral variants that do not respond to virally targeted therapies.

Subgenomic 1B HCV RNA replicon

The first replicon system of HCV was established by the Lohmann et al. and was termed Subgenomic 1B HCV RNA replicon (Fig. 2). This replicon system specifically focuses on replication as it only encodes the minimal amount of HCV proteins required for replication (NS3-5B) driven by an EMCV IRES and no structural proteins. The structural genes are replaced by a *neomycin* resistance cassette driven by the HCV IRES (Fig. 2) (Lohmann et al., 1999). All of the genes are flanked by the HCV 5' and 3'UTR (Fig. 2). The replicon is utilized by nicking of the replicon plasmid and subsequent *in vitro* translation with an upstream T7 polymerase promoter site. The resulting RNA-based replicons are transfected into hepatocyte cell line Huh7 (Fig. 2). Unfortunately, only a small percentage of Huh7 cell are able to support the replication of HCV virus demonstrating that Huh7 cells are not permissive for viral replication. As a result, neomycin selection is used to promote the growth of cells that are able to support viral replication (Blight et al., 2002; Lohmann et al., 1999).

In an effort to establish cell lines that were permissive for viral replication, a strategy was developed for the enrichment of the existing permissive cells in the Huh7 line. After replicon transfection and selection with neomycin, colonies were picked and treated with interferon to "cure" these cells of HCV replicon. If these cells were re-transfected with replicon, they are found to robustly support HCV replication. In this manner, the first permissive cell line, Huh7.5, was established (Blight et al., 2002).

After the establishment of the permissive Huh7.5 line, comparisons between the non-permissive parental line, Huh7, and the permissive Huh7.5 line were performed to determine host factors that were lost in the permissive line that contribute to the increased permissiveness observed in Huh7.5. These studies led to the discovery of RIG-I, a sensor of double-stranded RNA that stimulates an interferon response (Sumpter et al., 2005). Work by Sumpter et al. found Huh7.5 cells contained a point mutation in RIG-I that renders it non-functional. As a result, Huh7.5 cells do not have an interferon response when challenged with viral infection (Sumpter et al., 2005). However, knockdown of RIG-I in the parental Huh7 line did not lead to the expected increase in HCV replication (Binder et al., 2007). These data suggest that there are other factors lost from the Huh7.5 cell line that contributes to the increased permissiveness of this line. By comparing non-permissive Huh7 to permissive lines generated as outlined here, CREB3L1 is identified as a host factor that limits HCV replication (See Chapter 2).

CREB3L1 discovery and role in bone development

CREB3L1 was originally discovered in astrocytes and coined OASIS (Old-Astrocyte Specifically Induced Substance). CREB3L1 mRNA expression was found to

be up-regulated during brain development and after cryo-injury, but further function was undetermined in the study (Honma et al., 1999). In a later study, *in situ* analysis of mouse tissue found CREB3L1 mRNA was highly expressed in developing osteoblasts suggesting a role in bone development (Nikaido et al., 2001). In fact, CREB3L1 genetic knock-out mice show a decrease in bone density which further substantiates the claim of CREB3L1 involvement in bone development (Murakami et al., 2009). The function of CREB3L1 in other tissues or outside of bone development is unknown.

Regulated Intramembrane Proteolysis

CREB3L1 is a membrane-bound transcription factor that is thought to localize to the endoplasmic reticulum (ER). In response to appropriate stimuli, CREB3L1 has been shown to translocate to the golgi and undergo Regulated Intramembrane Proteolysis (RIP) (Murakami et al., 2006). The prototype protein for which RIP was characterized is SREBP2 in response to a lack of cholesterol (Ye et al., 2000a). Later, ATF6 was also characterized to undergo RIP in response to ER stress (Ye et al., 2000b). These transcription factors are synthesized as membrane-bound precursors that contain at least one transmembrane helix with their transcriptional activation NH_2-terminal domain facing the cytosol. RIP is mediated by two golgi-localized proteases termed Site 1 Protease (S1P) and Site 2 Protease (S2P). Without stimulation, the membrane-bound transcription factors are localized to the ER and are separated from the proteases. Upon stimulation the membrane-bound transcription factors are transported to the golgi and activated by two sequential cleavages mediated by Site-1 protease (S1P) and Site-2 protease (S2P). The S1P catalyzed cleavage at the lumenal side is a prerequisite for the

S2P-catalyzed intramembrane cleavage. S1P cleaves at a RXXL sequence motif in the luman of the golgi. Once S1P has cleaved the substrate, S2P may cleave in the plain of the membrane. S2P cleavage requires a helix-breaking sequence such as PXXP in the transmembrane segment. After S2P cleavage, the NH2-terminal domains of the protein are released from the membranes, allowing them to enter the nucleus where they drive the transcription of their downstream genes (Fig. 4) (Brown et al., 2000).

Previous studies show CREB3L1 undergoes RIP in response to drugs that induce ER stress such as tunicamycin and thapsigargin (Murakami et al., 2006). Induction of CREB3L1 RIP has also been demonstrated to be stimulated by Bone Morphogenetic Protein 2 (BMP2) in osteoblasts to activate transcription of type I collagen, a direct target gene of CREB3L1 (Murakami et al., 2009). No study has been conducted to determine the role of CREB3L1 in other cell types with other ER stress-inducing conditions such as viral infection. Aside from collagen, no other downstream genes have been determined for CREB3L1.

Possible role of CREB3L1 in viral response

Viral infection is known to cause ER stress due to the massive expression of viral proteins (He, 2006; Medigeshi et al., 2007; Tardif et al., 2002). While no direct testing has been performed to determine if CREB3L1 is cleaved during viral infection, some evidence exists that CREB3L1 could be involved in anti-viral response. One study has shown a reduction in the expression level of CREB3L1 in West Nile Virus infected patients (van Marle et al., 2007). If CREB3L1 does have a role in controlling viral infection, it would be conceivable that viruses would seek to reduce CREB3L1

expression levels. No previous data exists on exactly how CREB3L1 could limit viral replication.

Role of CREB3L1 in cancer development

Several case reports are published for the presence of CREB3L1 chromosomal rearrangements in fibromyxoid sarcomas and one case in a small cell osteosarcoma (Debelenko et al., 2011; Mertens et al., 2005; Moller et al., 2011). All cases report a CREB3L1 fusion transcript with other genes such as the *FUS* gene (Mertens et al., 2005) or the *EWSR* gene (Debelenko et al., 2011). While a chimera protein containing the CREB3L1 bZiP DNA-binding domain is expressed, the role of this chimeric protein in cancer is unclear. Published reports tend to suggest the fusion protein causes the cancer. The possibility also exist that disruption of normal CREB3L1 function leads to cancer.

Scope of current study

The scope of this study is to characterize the function of CREB3L1 as it relates to viral infection and to determine the potential role of CREB3L1 in anti-cancer therapy. Chapter 2 will focus on the role of CREB3L1 in viral infection. Chapter 3 will demonstrate the correlation of CREB3L1 expression with the effectiveness of an anti-cancer drug, doxorubicin.

Chapter 1 Figures

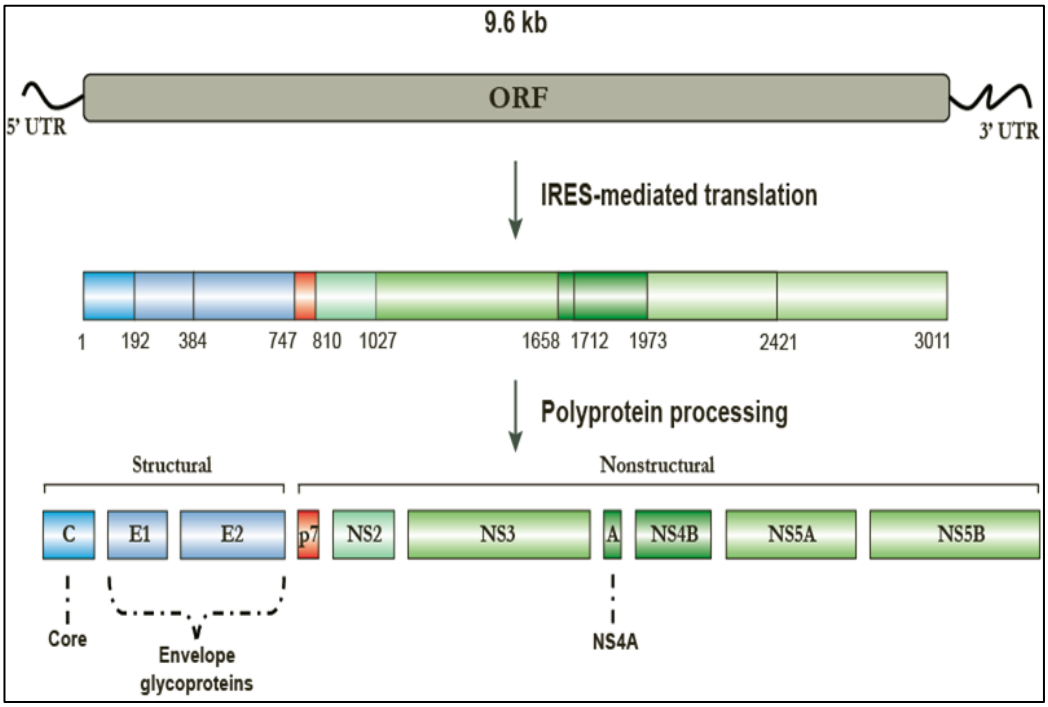

Figure 1. Genomic structure and polyprotein processing of HCV
HCV contains a single open reading frame flanked by a 5' and 3' UTR. The polyprotein is translation is mediated by an IRES site in the 5'UTR. The polyprotein is then processed by host peptidases and viral proteases into the 10 major HCV proteins [Figure modified from (Tse, 2010)].

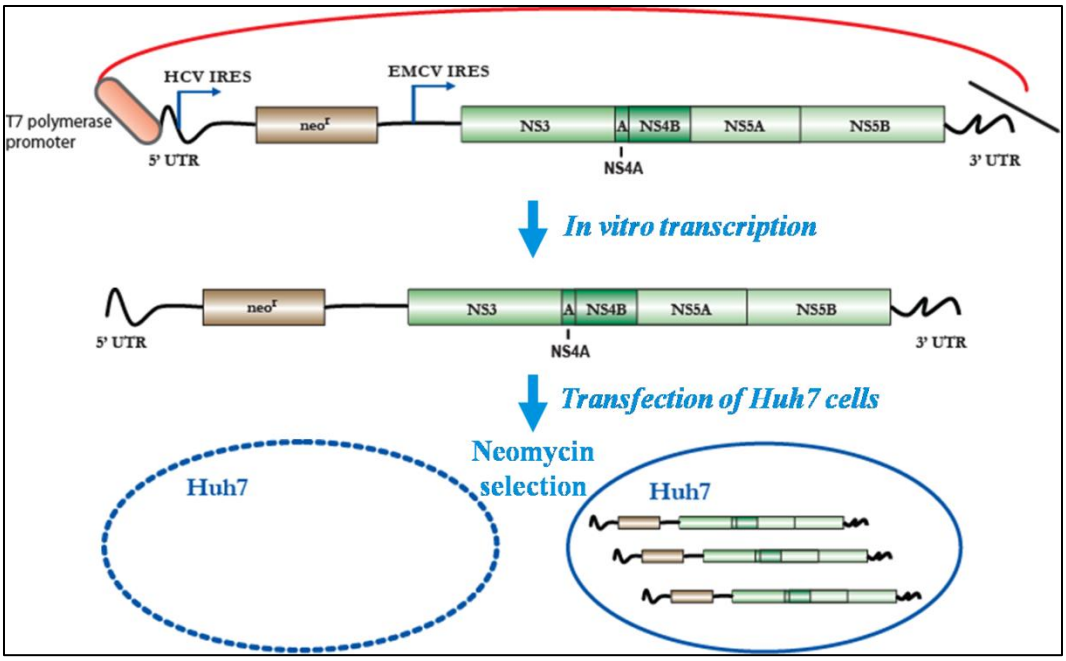

Figure 2. Subgenomic 1B HCV Replicon system
The Subgenomic 1B HCV Replicon system consists of minimal HCV proteins required for replication (NS3-5B). HCV structural proteins are replaced with a neomycin resistance gene. All genes are flanked by the 5' and 3'UTR. RNA-based replicon is generated by nicking the plasmid-based replicon and performing *in vitro* transcription utilizing an upstream T7 polymerase promoter. The transcribed RNA-based replicon is then transfected into Huh7 cells that are placed under selection for clones that support replication of HCV.

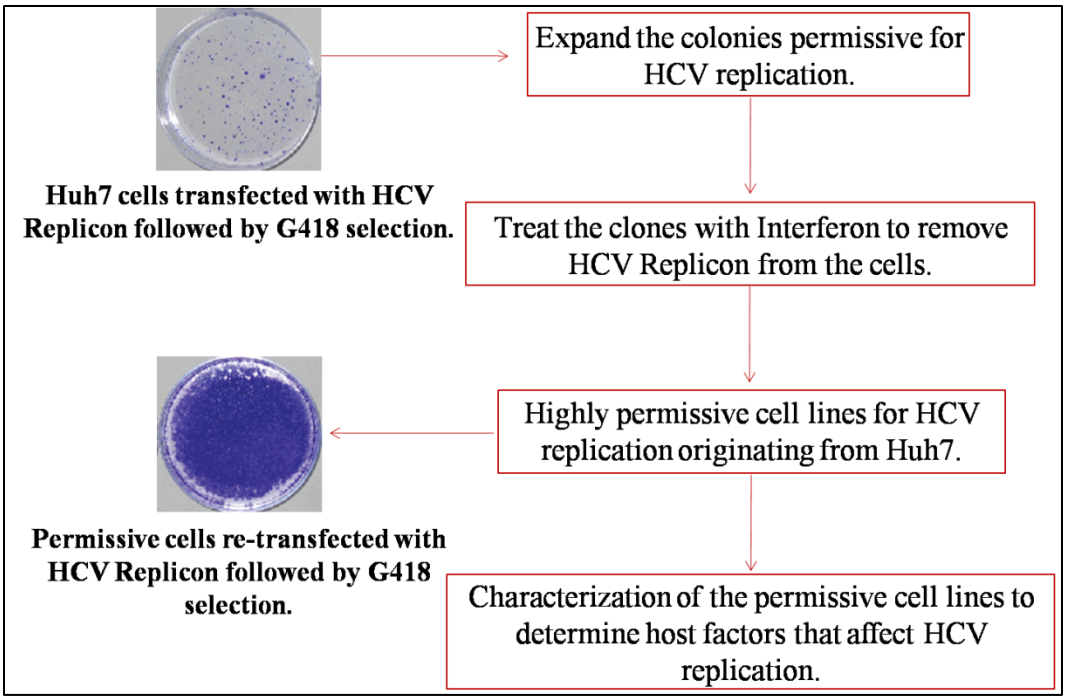

Figure 3. Flow-chart describing the enrichment of HCV replication permissive cells Huh7 clones that survive selection are expanded and treated with interferon to remove the HCV replicon. Upon re-transfected with HCV replicon, these cells are very permissive for viral replication. The newly generated permissive lines can then be compared to the non-permissive Huh7 line to determine host factors that affect viral replication.

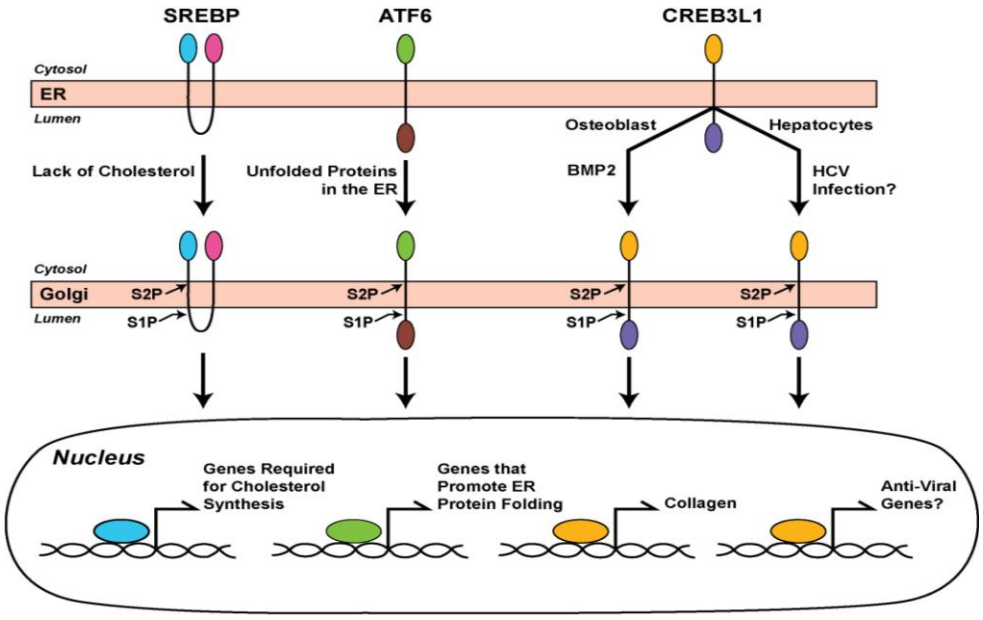

Figure 4. Regulated Intramembrane Proteolysis of membrane-bound transcription factors

In the presence of cholesterol, SREBP normally resides on the ER. When cells are depleted of cholesterol, SREBP traffics to the golgi where it is cleaved sequentially by S1p and S2P. This cleaved releases the NH_2-terminal portion of the protein so that it may enter the nucleus to drive genes required for cholesterol synthesis. ATF6 is trafficked to the golgi in response to unfolded proteins in the ER. Like SREBP, it is cleaved and nuclear localized to drive chaperone genes. CREB3L1 was previously reported to undergo RIP in response to BMP2 to generated collagen. It is unknown if HCV infected will trigger CREB3L1 cleavage via RIP and what genes it would transcribe.

Chapter 2: CREB3L1 blocks proliferation of virus-infected cells

INTRODUCTION

In the current study, we identify cAMP response element binding protein 3-like 1 (CREB3L1, also known as OASIS) as a cellular transcription factor expressed in parental Huh7 cells, but not in Huh7.5 cells and another subclone of Huh7 cells that are different from Huh7.5 cells but also highly permissive for HCV replication (HRP-1). CREB3L1 belongs to a family of transcription factors that are synthesized as membrane-bound precursors in the endoplasmic reticulum (ER). In response to stimulation, the protein is transported to the Golgi, where they are activated through regulated intramembrane proteolysis (RIP) (Brown et al., 2000; Murakami et al., 2006). In osteoblasts, ER stress triggers RIP of CREB3L1 by S1P and S2P, and the nuclear fragment activates the gene encoding type 1 collagen (Murakami et al., 2009). The function of CREB3L1 in other cells is unknown. Here, we show that CREB3L1 is proteolytically activated in cells infected by HCV or other RNA and DNA viruses to block proliferation of these cells by inducing transcription of genes encoding inhibitors to the cell cycle. As a result, CREB3L1 must be silenced in proliferating cells that support viral replication.

RESULTS

CREB3L1 Inhibits HCV Replication

While a mutation in RIG-I helps to render Huh7.5 more susceptible to HCV infection, this mutation may not be sufficient to cause permissiveness for HCV replication. We found that knockdown of RIG-I by RNAi did not enhance replication of

HCV in Huh7 cells (Figure 5A). A similar result was also observed previously (Binder et al., 2007) . Thus, it is likely that Huh7.5 cells may have altered expression of other genes that limit HCV replication. We sought to identify these genes by comparative microarray analysis of Huh7 and Huh7.5 cells. These experiments were inconclusive, due to the large number of genes differentially expressed between these cells. To narrow the candidate genes, we needed an independent line of Huh7 cells also permissive for HCV replication, so that we might identify genes with reduced expression in both lines of permissive cells. For this purpose, we treated Huh7-K2040 cells, a line of Huh7 cells that harbor an HCV replicon (Ye et al., 2003), with interferon to obtain a clone of cured Huh7 cells that no longer contained HCV RNA. HCV replicon RNA was then retransfected into these cells to determine their permissiveness for HCV replication. Similar to Huh7.5 cells, these cells were more permissive for HCV replication than their parental Huh7 cells, as measured by the number of colonies that contain the HCV replicon encoding the *neo* (Figure 5B) or by the activity of luciferase encoded by an HCV replicon RNA that contains the luciferase sequence in lieu of *neo* (Vrolijk et al., 2003) (Figure 5C). We named the cured Huh7-K2040 cells HCV replication-permissive (HRP-1) cells. Unlike Huh7.5 cells, HRP-1 cells do not contain a mutation in RIG-I, and they were not defective in activating interferon induced genes after infection with Sendai virus (Figure 5D) suggesting that RIG-I may not be that central host factor that allows HCV replication in permissive cell lines.

Microarray analysis revealed 26 genes whose expression was reduced by more than 10-fold in both HRP-1 and Huh7.5 cells compared to the parental Huh7 cells (Table 1). Among these genes, we chose to focus on CREB3L1, because infection with West

Nile virus (WNV), another flavivirus, was known to reduce the amount of this protein in neurons (van Marle et al., 2007).

Quantitative real-time PCR (real-time QPCR) analysis showed that the expression of CREB3L1 was reduced by more than 10-fold in both Huh7.5 and HRP-1 compared to the parental Huh7 cells (Figure 6A). Expression of CREB3L1 was also reduced in Huh7-K2040 cells, the progenitor for HRP-1 cells that harbors an HCV replicon (Figure 6A). Immunoblot analysis confirmed the difference in the amount of CREB3L1 protein among these cells (Figure 6B). We then determined whether the lack of expression of CREB3L1 renders cells permissive for HCV replication. CREB3L1 was markedly knocked down by siRNAs targeting two different regions of CREB3L1 mRNA (Figure 6C). Treatment of Huh7 cells with these siRNAs raised the amount of HCV replicon RNA replicated in the cells (Figure 6D). To study the replication of live virus, we used the JFH strain of HCV, the only strain of the virus that infects cultured cells (Wakita et al., 2005). We used Huh7.5 instead of Huh7 or HRP-1 cells because the latter cells were not infected by the virion, possibly owing to their intact interferon responses. Although Huh7.5 cells are already permissive for HCV replication and express less CREB3L1 compared to Huh7 cells, knockdown of CREB3L1 by RNAi led to a further increase in HCV RNA after these cells were infected by the HCV virion (Figure 6E).

To determine whether overexpression of CREB3L1 inhibits HCV replication, we transfected CREB3L1 into Huh7-K2040 cells. Due to the problem of low transfection efficiency, we subcloned CREB3L1 into a plasmid that also expresses GFP (pTracer). We used a fluorescence-activated cell sorter (FACS) to isolate cells that expressed GFP and CREB3L1 (Figure 6F, lane 4). CREB3L1 displayed two bands as a result of

proteolytic cleavage (see below). The amount of NS5A, an HCV protein whose expression depends on viral replication (Ye et al., 2003), was markedly reduced in these cells (Figure 6F, lane 4). This effect was not due to the expression of GFP because transfection of the empty pTracer encoding GFP, but not CREB3L1, did not reduce the amount of NS5A (Figure 6F, lane 2). To determine the effect of CREB3L1 overexpression on infection of the HCV virion, we transfected Huh7.5 cells with pTracer-CREB3L1 or the pTracer vector, isolated transfected cells through FACS, and infected these cells with the HCV virion. As shown in Figure 6G, overexpression of CREB3L1 also reduced the amount of HCV RNA in Huh7.5 cells infected by the HCV virion.

CREB3L1 Is Proteolytically Activated in Cells Harboring HCV Replicon

CREB3L1 contains a recognition sequence for S1P (RXXL located within 30 residues from the transmembrane helix) (Hua et al., 1996) and S2P (helix-breaking sequences, such as PXXP, in the transmembrane helix) (Ye et al., 2000a) (Figure 7A). To determine whether RIP of CREB3L1 is induced in hepatoma cells by HCV infection, we transfected a plasmid encoding CREB3L1, tagged at the NH2 terminus with an epitope derived from herpes simplex virus (HSV), into Huh7, HRP-1, and Huh7-K2040 cells. The expression of CREB3L1 encoded by the plasmid was driven by the weak thymidine kinase (TK) promoter to avoid constitutive cleavage of the protein caused by excessive overexpression. The amount of full-length CREB3L1 and the NH2-terminal fragment of CREB3L1 was detected by anti-HSV, which is sensitive enough to detect transfected proteins driven by the TK promoter in immunoblot analysis (Hua et al., 1996). In Huh7 and HRP-1 cells, which do not contain an HCV replicon, we observed only the full-

length precursor of CREB3L1, with a molecular weight of ~80 kDa in the membrane fraction (Figure 7B, lanes 2 and 6). Cleaved CREB3L1 was not detectable in the nuclear fraction (Figure 7B, lanes 2 and 6). In Huh7-K2040 cells, which contain an HCV replicon, the cleaved NH2-terminal fragment of CREB3L1 (nuclear form, ~55 kDa) was prominent in the nuclear fraction (Figure 7B, lane 4). In these cells, generation of the nuclear form was reduced when we transfected plasmids encoding CREB3L1 with mutations that disrupt the consensus S1P (R423A) or S2P recognition site (P392A/P395A) (Figure 7C, lanes 2–4). When the S2P recognition site was altered, we observed in the membrane fraction a cleaved fragment with a molecular weight similar to the nuclear form (Figure 7C, lane 4). This fragment is the membrane-bound intermediate form of CREB3L1 that is cleaved by S1P, but not by S2P. A similar cleavage intermediate was observed for SREBP-2, a prototype of RIP substrates, when its S2P recognition site was disrupted (Ye et al., 2000a). These results suggest that CREB3L1 is activated through RIP in HCV-infected cells.

To determine whether production of the nuclear CREB3L1 is sufficient to inhibit HCV replication, we transfected Huh7-K2040 cells with a plasmid encoding the truncated NH2-terminal domain of CREB3L1 (CREB3L1[Δ381–519]), which enters the nucleus without cleavage. Overexpression of CREB3L1(Δ381–519) also inhibited HCV replication in Huh7-K2040 cells as indicated by NS5A expression (Figure 7D). This effect was not observed when the DNA-interacting bZIP domain (Figure 7A) was deleted from the nuclear CREB3L1 (CREB3L1[Δ 290–519]) (Figure 7E), even though deletion of this domain did not prevent nuclear localization of the protein (Figure 8). These results

suggest that the nuclear CREB3L1 is likely to activate transcription of genes that inhibit viral replication.

Nuclear CREB3L1 Blocks Cell Proliferation

To identify genes activated by CREB3L1, we transfected Huh7-K2040 cells with CREB3L1(Δ 381–519) subcloned into pTracer and used FACS to isolate cells that expressed GFP and CREB3L1. Microarray analysis was performed to compare gene expression between these cells and cells transfected with the empty pTracer plasmid. In addition to collagen 1a1, a known target of CREB3L1 (Murakami et al., 2009), CREB3L1(Δ381–519) also activated transcription of a group of genes that inhibit the cell cycle (Table 2). These genes encode cyclin inhibitors p21 and p18 (Sherr and Roberts, 1999), c-myc antagonists Mxi-1 (Hurlin and Huang, 2006), and other proteins known to inhibit cell proliferation, such as GADD45γ (Liebermann and Hoffman, 2002), SPARC (Bradshaw and Sage, 2001), and RGC32 (Saigusa et al., 2007). Real-time QPCR analysis confirmed that all of these genes were induced by CREB3L1(Δ381–519) (Figure 9A). Despite this induction, none of the 5'-flanking regions of these genes contains the nucleotide sequences reported to bind CREB3L1 (Kondo et al., 2005; Murakami et al., 2009). To identify the CREB3L1 response element in these cell-cycle-inhibitory genes, we performed reporter assays using a luciferase reporter gene driven by a 2 kb fragment of the 5'-flanking region of p21. Luciferase activity was markedly enhanced (~20-fold) by CREB3L1(Δ381–519) transfected into Huh7-K2040 cells (Figure 9B). Serial deletion analysis indicated that a segment encompassing nucleotide positions -40 to -16 relative to the transcription start site of p21 conveyed CREB3L1 inducibility (Figure 9B). Sequence

analysis revealed that position -34 to -26 within this fragment contains a consensus sequence GTGXGCXGC that is conserved in promoters of all genes activated by CREB3L1 (Figure 9C). Deletion of this sequence or the changing of all nucleotides in the sequence to adenines reduced the ability of CREB3L1 to stimulate luciferase activity (Figure 9D). An artificial promoter containing only the consensus sequence (repeated three times) was activated by CREB3L1 (Figure 9D). Chromatin Immunoprecipitation (ChIP) assays revealed that FLAG-tagged CREB3L1(Δ381–519) bound to the promoter region of endogenous p21 (Figure 9E, lane 6). Deletion of the bZIP domain from the NH2-terminal segment of CREB3L1 (CREB3L1[Δ290–519]) abolished this interaction (Figure 9E, lane 4) while transfection of empty vector (Figure 9E, lanes 1-2) or pulldown with a non-specific IgG (Figure 9E, lanes 1, 3, & 5) did not yield the correct size band.

The above results suggest that the nuclear form of CREB3L1 inhibits cell-cycle progression by binding to promoters and activating transcription of genes encoding cell-cycle inhibitors. To test this hypothesis, we transfected Huh7-K2040 cells with CREB3L1(Δ381–519) subcloned into pTracer, incubated the cells for 3 days to allow these cells to divide, and quantified the number of cells containing the plasmid by FACS. The number of GFP-positive cells was 4-fold less in cells transfected with pTracer-CREB3L1(Δ381–519) than those transfected with the empty pTracer (Figure 10A), suggesting that CREB3L1(Δ381–519) inhibited cell proliferation. This effect was not observed when Huh7-K2040 cells were transfected with the nuclear CREB3L1 in which bZIP domain is deleted (CREB3L1[Δ290–519]) (Figure 10A).

To more directly access the role of CREB3L1 in cell proliferation, we performed time-lapse imaging analysis of Huh7-K2040 cells transfected with the NH2-terminal

fragment of CREB3L1 subcloned into pTracer. At the end of the experiment, GFP fluorescent images were taken to identify cells transfected with the plasmid, and these cells were traced backward to determine if they underwent division events. Representative time-lapse images of Huh7-K2040 cells transfected with pTracer - CREB3L1(Δ381–519), pTracer-CREB3L1(Δ290–519), or the pTracer vector are shown in Figure 10B. Quantitative analysis of these images indicated that more than 70% of cells transfected with the empty pTracer went through at least one cycle of cell division during a period of 48 hr (Figure 10C). Less than 20% of cells transfected with pTracer-CREB3L1(Δ381–519) divided during the same period (Figure 10C). Deletion of the bZIP domain in CREB3L1 (CREB3L1(Δ290–519)) abolished the inhibition of cell division (Figure 10C).

The data presented above indicate that HCV infection induces the processing of CREB3L1 to its nuclear form, which in turn suppresses cell-cycle progression by coordinately activating a host of genes encoding proteins that inhibit the cell cycle. Since active division of host cells is known to be required for efficient HCV replication (Pietschmann et al., 2001; Scholle et al., 2004), we conclude that the nuclear form of CREB3L1 suppresses HCV replication by blocking the cell cycle. In order for cells to become permissive for HCV replication, CREB3L1 must be silenced, as in Huh7.5 and HRP-1 cells, so that these cells are able to divide after they are infected by HCV.

CREB3L1 Blocks Proliferation of Cells Infected by Viruses Other than HCV

To determine the role of CREB3L1 in viruses other than HCV, we examined the expression of the gene in Huh7-WNV2 cells, a line of a Huh7 cells harboring a replicon

of WNV, another flavivirus (Wang et al., 2005). We observed that expression of CREB3L1 is markedly reduced in these cells, compared to the parental Huh7 cells, as determined by real-time QPCR (Figure 11A) and immunoblot analysis (Figure 11B). CREB3L1 was cleaved to produce the nuclear form upon transfection into Huh7-WNV2 but not Huh7 cells (Figure 11C). Unlike HCV, replication of WNV was not affected by overexpression of the nuclear form of CREB3L1 (data not shown). This result suggests that unlike HCV, replication of WNV may not depend on active division of host cells. To test this hypothesis, we incubated Huh7 cells harboring an HCV or WNV replicon with hydroxyurea, a drug that inhibits the cell cycle by blocking DNA synthesis (Ye et al., 2003) While reducing the amount of HCV RNA, the drug treatment did not affect the amount of WNV RNA (Figure 11D). However, overexpression of the nuclear form of CREB3L1 still led to suppression of cell division in Huh7-WNV2 cells (Figure 11E). This result might explain why CREB3L1 has to be silenced in Huh7-WNV2 cells, as these cells have to proliferate in the presence of persistent replication of WNV genome.

To determine whether the effect of CREB3L1 is restricted to flavivirus, we examined the role of CREB3L1 in inhibiting proliferation of cells infected by Sendai virus, a negative-stranded RNA virus of Paramyxoviridae. Infection of Huh7 cells with Sendai virus stimulated the cleavage of CREB3L1 (Figure 12A). Infection of Sendai virus almost completely blocked proliferation of Huh7 cells, which express CREB3L1 (Figure 12B). The proliferation of HRP-1 cells, which do not express CREB3L1, was not affected by the viral infection (Figure 12B). Huh7-shCREB3L1 cells, which were generated by stably transfecting Huh7 cells with a shRNA targeting CREB3L1, produced much less CREB3L1 mRNA (Figure 13A). Proliferation of these cells was also not

affected by the Sendai virus infection (Figure 12B). The failure of Sendai virus to inhibit proliferation of HRP-1 and Huh7-shCREB3L1 cells was not caused by less efficient infection of the cells by the virus, as the amount of viral RNA in these cells was even more than that in Huh7 cells (Figure 12C). Sendai virus did not lyse the cells in the experiments as there was no lactate dehydrogenase activity detected in the culture medium. Similar to WNV, replication of Sendai virus does not require proliferation of host cells, as hydroxyurea treatment did not inhibit replication of the viral RNA (Figure 13B).

To investigate the role of CREB3L1 in defending against infection of DNA virus, we infected Huh7 cells with murine g-herpesvirus 68 (MHV-68). The genome of MHV-68 we used also encodes GFP that serves as a marker for viral infection (Dong et al., 2010). As with Sendai virus, infection of Huh7 cells with MHV-68 also triggered the cleavage of CREB3L1 (Figure 12D). Infection with MHV-68 blocked the proliferation of Huh7 cells (Figure 12E). Proliferation of HRP-1 and Huh7-shCREB3L1 cells, which express much less CREB3L1 compared to the parental Huh7 cells, was not affected by the viral infection (Figure 12E). The lack of CREB3L1 did not affect viral infection, as expression of GFP encoded by MHV-68 was the same in Huh7, HRP-1, and Huh7-shCREB3L1 cells (Figure 12F).

To determine the function of CREB3L1 in cells that are not derived from Huh7 cells,we infected SV589 cells, an immortalized line of human fibroblasts (Yamamoto et al., 1984), with Sendai virus. The viral infection stimulated the cleavage of CREB3L1 in SV589 cells (Figure 13C). Sendai virus infection reduced the rate of proliferation of SV589 cells transfected with the control siRNA, but not those transfected with the siRNA

targeting CREB3L1 (Figure 13D), which decreased the amount of CREB3L1 mRNA by ~90% (Figure 13E). Knockdown of CREB3L1 did not alter the amount of viral RNA in SV589, suggesting that the failure of Sendai virus to inhibit proliferation of SV589 cells in which CREB3L1 was knocked down was not caused by less efficient infection of the cells by the virus (Figure 13F).

DISCUSSION

The results presented above support a model shown in Figure 14. CREB3L1 is synthesized as a membrane-bound precursor. In cells infected by a DNA virus such as MHV-68, negative-stranded RNA viruses such as Sendai virus, or positive-stranded RNA viruses such as HCV and WNV, CREB3L1 is activated by RIP catalyzed by S1P and S2P. As an analogy to other well- characterized transcription factors activated through RIP, we assume that the viral infection stimulates the translocation of CREB3L1 precursor from the ER to the Golgi complex in which S1P and S2P reside (DeBose-Boyd et al., 1999; Shen et al., 2002). Following the cleavage, the NH2-terminal domain of CREB3L1 enters the nucleus, where it activates transcription of genes encoding cell-cycle inhibitors to block proliferation of the virus-infected cells. For most of the viruses we analyzed, inhibition of proliferation of their host cells did not affect their replication.

Thus, rather than directly inhibiting viral replication, CREB3L1 may play an important role in preventing virus spread by limiting proliferation of virus-infected cells. Among the viruses we studied, HCV is unique in that its replication in Huh7-derived cells requires active division of the host cells (Pietschmann et al., 2001; Scholle et al., 2004). As a result, CREB3L1-mediated signaling not only blocks proliferation of virus-infected

cells, but also inhibits HCV replication. However, the in vivo relevance of the observation remains to be determined. Although hepatocytes do not enter the cell cycle in healthy livers, they proliferate rapidly to repair liver injuries induced by HCV infection. Thus, further studies are required to determine whether CREB3L1 inhibits division of virus-infected hepatocytes in vivo to limit HCV replication at a low level and to prevent the spread of the virus.

It was reported previously that ER stress triggers cleavage of CREB3L1 (Murakami et al., 2006). ER stress is also known to be induced by massive synthesis of ER-associated viral proteins in cells infected by viruses (He, 2006). These viruses include those used in the current study, such as HCV (Tardif et al., 2002; von dem Bussche et al., 2010) and WNV (Medigeshi et al., 2007). Thus, it is conceivable that viral infection triggers cleavage of CREB3L1 through ER stress. If this is the case, CREB3L1 may belong to a growing list of proteins that defend against viral infection through ER stress (Martinon and Glimcher, 2011).

In the current study, we show that both Huh7.5 and HRP-1 cells are highly permissive for replication of HCV subgenomic replicons derived from the genotype 1 HCV, owing to the lack of expression of CREB3L1. However, only Huh7.5 but not HRP-1 cells can be infected by the JFH1 strain of the genotype 2 HCV. Unlike genotype 1 HCV, genotype 2 HCV is much more sensitive to interferon (Zein, 2000). This difference between Huh7.5 and HRP-1 cells might be explained by a mutation in RIG-I found in Huh7.5 (Sumpter et al., 2005), but not in HRP-1 cells, which makes Huh7.5 but not HRP-1 cells defective in producing interferon in response to viral infection.

Since CREB3L1 inhibits cell proliferation by activating genes encoding proteins that inhibit the cell cycle, it may be considered as a tumor suppressor gene. Indeed, inactivation of CREB3L1 through chromosome fusion is associated with development of low-grade fibromyxoid sarcoma (Mertens et al., 2005). Considering that CREB3L1 is proteolytically activated in virus-infected cells, the protein may play an important role in preventing virus-induced tumorigenesis. Notably, the ability of CREB3L1 to inhibit cell proliferation has not been observed in previous studies that analyze genes activated by the protein (Fox et al., 2010; Kondo et al., 2005; Murakami et al., 2009; Vellanki et al., 2010). Unlike the current study, these analyses were not performed in virus-infected cells. We observed that the nuclear form of CREB3L1 activated genes that suppress cell proliferation much more profoundly in Huh7-K2040 cells that harbor an HCV replicon than the naive Huh7 cells (data not shown). Thus, it is likely that another factor generated in virus infected cells cooperates with the nuclear form of CREB3L1 to activate these genes.

In addition to genes encoding proteins that inhibit the cell cycle, CREB3L1 also activates transcription of type 1 collagen and genes involved in assembly of collagen matrix as previously reported (Murakami et al., 2009; Vellanki et al., 2010). This observation suggests that in addition to preventing proliferation of virus-infected cells, CREB3L1 may also limit the spread of the virus by activating production of small amounts of collagen in virus-infected cells to segregate these cells from their environment. Further study will be required to determine whether chronic deposition of collagen produced in virus-infected cells contributes to fibrosis induced by viral infection.

MATERIALS AND METHODS

Antibodies

We obtained rabbit anti-actin and anti-GFP from Abcam; mouse anti-HSV from Novagen; rabbit anti-LSD1 from Cell Signaling; mouse anti-calnexin from Enzo Life Sciences; peroxidase -conjugated secondary antibodies from Jackson ImmunoResearch. Rabbit anti-NS5A was described previously (Huang et al., 2007). A rabbit polyclonal antibody against human CREB3L1 was generated by immunizing rabbits with a protein consisting of the NH2-terminal 290 amino acid residues of human CREB3L1.

Cell Culture

Huh7, Huh7.5, HRP-1, and SV589 cells were maintained in medium A (Dulbecco's modified Eagle's medium with 4.5 g/l glucose, 100 U/ml penicillin, 100 mg/ml streptomycin sulfate, and 10% fetal calf serum). Huh7-K2040 cells were maintained in medium A supplemented with 200 mg/ml G418. Huh7-GL cells, a line of Huh7 cells that contain a chromosomally integrated JFH strain of HCV cDNA and constitutively produce infectious virus (Cai et al., 2005), were maintained in medium A supplemented with 5 mg/ml blasticidine. Huh7-shCREB3L1 cells were generated by stably transfecting a shRNA targeting CREB3L1 (SA Biosciences, Clone ID 2) into Huh7 cells. The cells were maintained in medium A supplemented with 10 mg/ml puromycin. All cells were cultured in monolayers at 37°C in 5% CO2.

Plasmids

pTracer-CMV (Invitrogen) is a plasmid that allows detection of transfected cells through expression of GFP encoded by the plasmid. pTracer-CREB3L1, pTracer-CREB3L1 (Δ381–519), and pTracer-CREB3L1(Δ290–519) encode CREB3L1 and its deletion mutants. pTK-HSV-CREB3L1 encodes full-length CREB3L1 preceded by two copies of the HSV epitope tag (QPELAPEDPED) at the NH2-terminus under the control of the TK promoter. pTK-HSV-CREB3L1(R423A) and pTK-HSV-CREB3L1 (P392A/P395A) were generated using the QuikChange II XL Site-Directed Mutagenesis Kit (Stratagene) with pTK-HSV-CREB3L1 as the template. pCMV-CREB3L1(Δ381–519) encodes a deletion mutant of CREB3L1 under the control of the CMV promoter. pCMV-FLAG-CREB3L1(Δ290–519) and pCMV-FLAG-CREB3L1(Δ381–519) encodes deletion mutants of CREB3L1 preceded with a FLAG epitope tag (DYKDDDDK) under control of a CMV promoter. For luciferase reporter experiments shown in Figures 5B and 5D, indicated regions of p21 promoter were cloned into pGL3 vector (Genescript).

Real-Time QPCR

Real-time QPCR was performed as previously described (Liang et al., 2002; Ye et al., 2003). Briefly, total RNA prepared from cells was treated extensively with DNase I (DNA-free, Ambion, Austin, TX). First-strand cDNA was synthesized from the DNA-free RNA by using random hexamer primers and the ABI cDNA synthesis kit (Applied Biosystems). cDNA was mixed with SYBR Green PCR Master Mix (Applied Biosystems) and sets of forward and reverse primers specific for the RNA subjected to the measurement and analyzed by real-time QPCR with the ABI PRISM 7900HT sequence

detection system (Applied Biosystems). All reactions were performed in triplicate. The relative amounts of RNAs were calculated through the comparative cycle threshold method by using human 36B4 mRNA as the invariant control.

Virus Infection

The JFH1 strain of HCV was produced from Huh7-GL cells, a gift from Guangxiang Luo (University of Kentucky), as previously described (Huang et al., 2007). The HCV HP or con1 replicon RNA was in vitro transcribed as previously described (Sumpter et al., 2004) and transfected into Huh7 cells using Trans-Messenger Reagent (QIAGEN). Sendai virus (Cantell strain) was purchased from Charles River Laboratories. The virus was added to cells after it was diluted 50-fold in cell-culture medium (3 ml/60 mm plate). MHV-68, a gift from Pinghui Feng (University of Texas Southwestern Medical Center), was used to infect the cells with a multiplicity of infection of 2 through spin infection, by spinning the cells at 1000 x g for 30 min.

RNA Interference

Duplexes of siRNA were synthesized by Dharmacon Research. The two siRNA sequences targeting human CREB3L1 (NCBI Accession number NM_052854) are at nucleotide positions (relative to the codon for the initiation methionine) 131–149 and 884–902, for CREB3L1-1 and CREB3L1-2, respectively. The control siRNA targeting GFP was reported previously (Adams et al., 2004). Cells were transfected with siRNA using Lipofectamine RNAiMAX reagent (Invitrogen) as described by the manufacturer, after which the cells were used for experiments as described in the figure legends.

Immunoblot Analyses to Determine RIP of CREB3L1

Cells were harvested and separated into nuclear and membrane fractions as described (Sakai et al., 1996). Four μg of nuclear fractions and 10 μg of membrane fractions were analyzed by 10% SDS-PAGE followed by immunoblot analysis with anti-HSV (0.25 mg/ml). Bound antibodies were visualized with a peroxidase-conjugated secondary antibody using the SuperSignal ECL-HRP substrate system (Pierce).

Isolation of Transfected Cells through FACS

Cells were trypsinized and sorted on a BD FACS Aria Flow Cytometer (Becton Dickinson) based on expression of GFP by the University of Texas Southwestern Flow Cytometry Core Facility. Sorted cells with or without GFP expression were then used for assays described in figure legends.

Luciferase Assays

Luciferase activity in the cell lysate was assayed with the Dual-Luciferase Reporter Assay system (Promega) using the Synergy 4 plate reader and Gen5 1.10 software (Biotek). Promoter activity was determined by firefly luciferase activity normalized against Renilla luciferase activity to control for transfection efficiency.

ChIP Analyses

ChIP was performed using the SimpleChiP Enzymatic Chromatin IP Kit (Cell Signaling Technology) according to the manufacturer's protocol. Genomic DNA was used for PCR

with the AccuPrime Pfx Supermix Kit (Invitrogen) using primers 5'AACTCGGCCAG GCTCAGCTG-3' and 5'GCTCCACAAGGAACTGACTTCGGCAG-3' to amplify a 200 bp segment of the p21 promoter. PCR products were run on a 2% agarose gel and imaged with the Eagle Eye II gel documentation system with EagleSight Software (Stratagene).

Time-Lapse Imaging

Cells were changed into CO2-Independent Medium (Invitrogen) supplemented with 10% FCS, 1% penicillin/streptomycin, 2 mM GlutaMAX (Invitrogen), and 1 mM sodium pyruvate for the imaging analysis. Phase contrast time-lapse imaging was performed with an Axiovert 200M (Ziess) microscope in a 37°C chamber, and images were taken every 10 minutes for 48 hr in at least four different fields per well using MetaMorph Software (Molecular Devices). GFP fluorescence images were taken at the end of the experiment at 48 hr. Cells transfected with different plasmids were imaged in parallel using a motorized stage (Marzhauser). Cells expressing GFP at 48 hr were traced backward to determine if these cells underwent division events.

Microarray Analysis

Microarray analysis was performed exactly as previously described (Horton et al., 2003).

Chapter 2 Figures

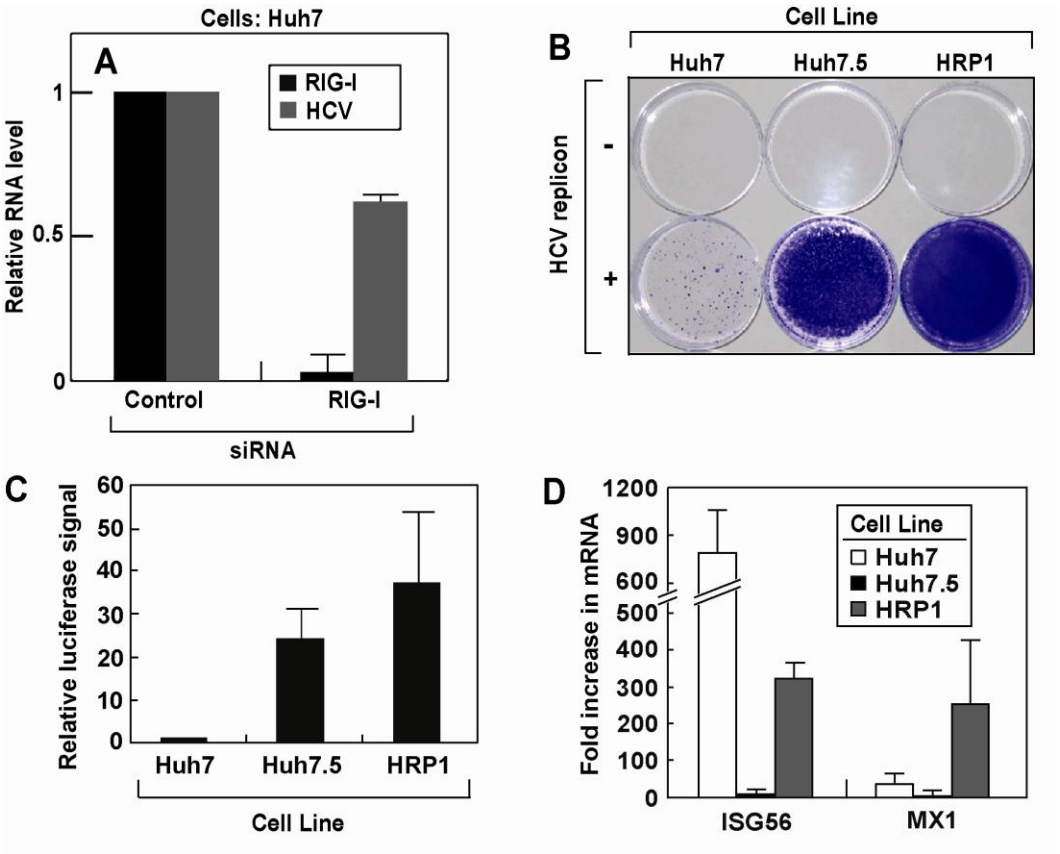

Figure 5. Characterization of HRP-1 Cells
(A) On day 0, Huh7 cells were seeded at 1×10^5/60 mm dish. On day 1, they were transfected with indicated siRNA (20 pmol/dish). On day 3, these cells were transfected with the HCV replicon RNA (HP, 0.5 μg/dish). On day 4, the cells were harvested and the amount of indicated RNA was quantified by RT-QPCR, with the amount of RNA in cells treated with the control siRNA set to 1. Results are reported as mean ± S.E. (n=2).
(B) On day 0, Huh7 cells, Huh7.5 cells and HRP-1 cells (cured Huh7-K2040 cells) were set up at 7×10^5/well in a 6-well plate. On day 1, they were transfected with HCV replicon RNA (con1, 1 μg/dish) as indicated. On day 2, cells were treated with 700 μg/ml G418. After two weeks of G418 selection, the cells were stained with crystal violet.
(C) On day 0, indicated cells were set up at 7×10^5/60mm dish. On day 1, they were transfected with an HCV replicon RNA in which the neomycin resistant gene was replaced by renilla luciferase (1 μg/dish) as well as a firefly luciferase RNA (1 μg/dish) driven by an EMCV IRES to control for transfection efficiency. On day 4, cells were harvested and the luciferase activity was measured. Relative luciferase activity is presented with the value of Huh7 cells set to 1.

(D) On day 0, indicated cells were set up at 7×105/60mm dish. On day 1, some of these cells were infected by Sendai virus. On day 2, cells were harvested and indicated mRNA was determined by RT-QPCR. Fold induction of indicated mRNA by Sendai virus infection is presented. Results are reported as mean ± S.D, (n=3) in (C) and (D).

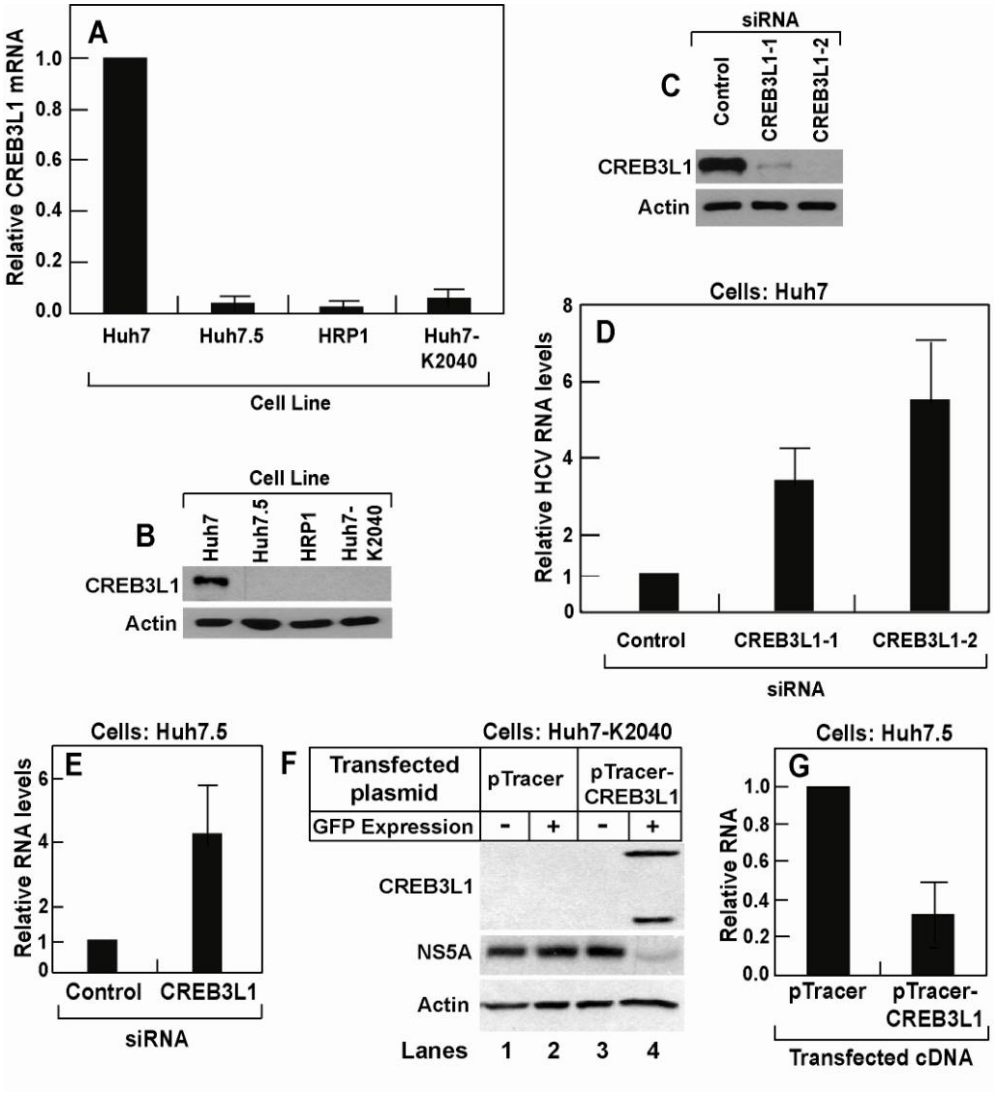

Figure 6. CREB3L1 Inhibits HCV Replication

(A) Real-time QPCR quantification of CREB3L1 mRNA in indicated cells with the value in Huh7 cells set to 1. (All panels) Bar graphs are reported as mean ± SD (n = 3).

(B) Immunoblot analysis of CREB3L1 protein in indicated cells.

(C and D) On day zero, Huh7 cells were seeded at 1 x 10^5/60 mm dish. On day one, they were transfected with indicated siRNA (20 pmol/dish). On day three, these cells were transfected with the HCV replicon RNA (HP, 0.5 μg/dish). On day four, the cells were harvested, and the amount of CREB3L1 protein was determined by immunoblot analysis (C). HCV RNA was quantified by real-time QPCR, with the amount of HCV RNA in cells treated with the control siRNA set to 1 (D).

(E) Huh7.5 cells were seeded and transfected with indicated siRNA as described in (C). On day three, the cells were infected with the JFH strain of HCV virion. On day four, the cells were harvested, and the amount of HCV RNA was quantified as described in (C).
(F) On day zero, Huh7-K2040 cells were seeded at 7 x 10^5/60 mm dish. On day one, they were transfected with 0.5 μg of a plasmid derived from pTracer as indicated. On day two, the cells were trypsinized and sorted through FACS based on expression of GFP. Lysates of the cells with or without GFP expression were subject to immunoblot analysis with indicated antibodies.
(G) Huh7.5 cells transfected with the indicated plasmid were isolated from untransfected Huh7.5 cells based on GFP expression, as described in (D), and seeded at 2 x 10^5/60 mm dish. They were infected by the JFH strain of HCV virion 24 hr later. Following incubation for 3 days, HCV RNA in the cells was quantified by real-time QPCR, with the value in cells transfected with the empty pTracer set at 1.

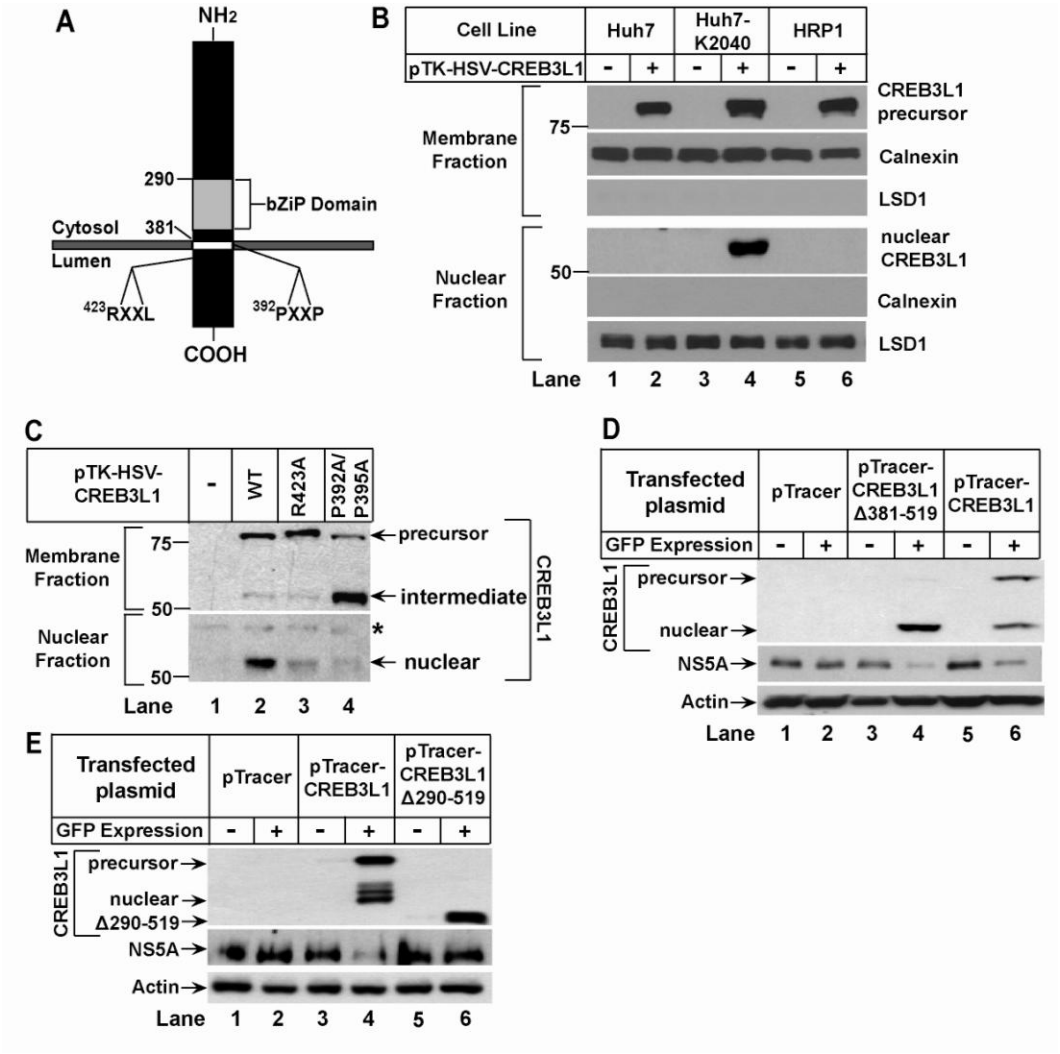

Figure 7. CREB3L1 Undergoes RIP in HCV-Infected Cells
(A) Schematic diagram of CREB3L1.
(B and C) On day zero, indicated cells (B) or Huh7-K2040 cells (C) were seeded at 4 x 10^5/60 mm dish. On day one, they were transfected with 50 ng of indicated plasmids. On day two, the cells were harvested and separated into nuclear and membrane fractions followed by immunoblot analysis with anti-HSV. Asterisk (*) denotes a cross-reactive band. Immunoblots of calnexin and Lysine-specific demethylase 1 (LSD1) served as loading controls for membrane and nuclear fractions, respectively.
(D and E) Huh7-K2040 cells transfected with the indicated plasmid were analyzed as described in Figure 2F.

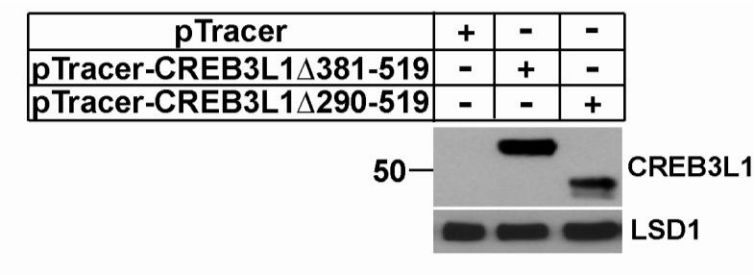

Figure 8. Nuclear Localization of CREB3L1(Δ290–519)
Huh7 cells were seeded and transfected with indicated plasmid as described in Figure 3B. The amount of COOH-terminal truncated CREB3L1 in the nuclear fraction was determined by immunoblot analysis with anti-CREB3L1.

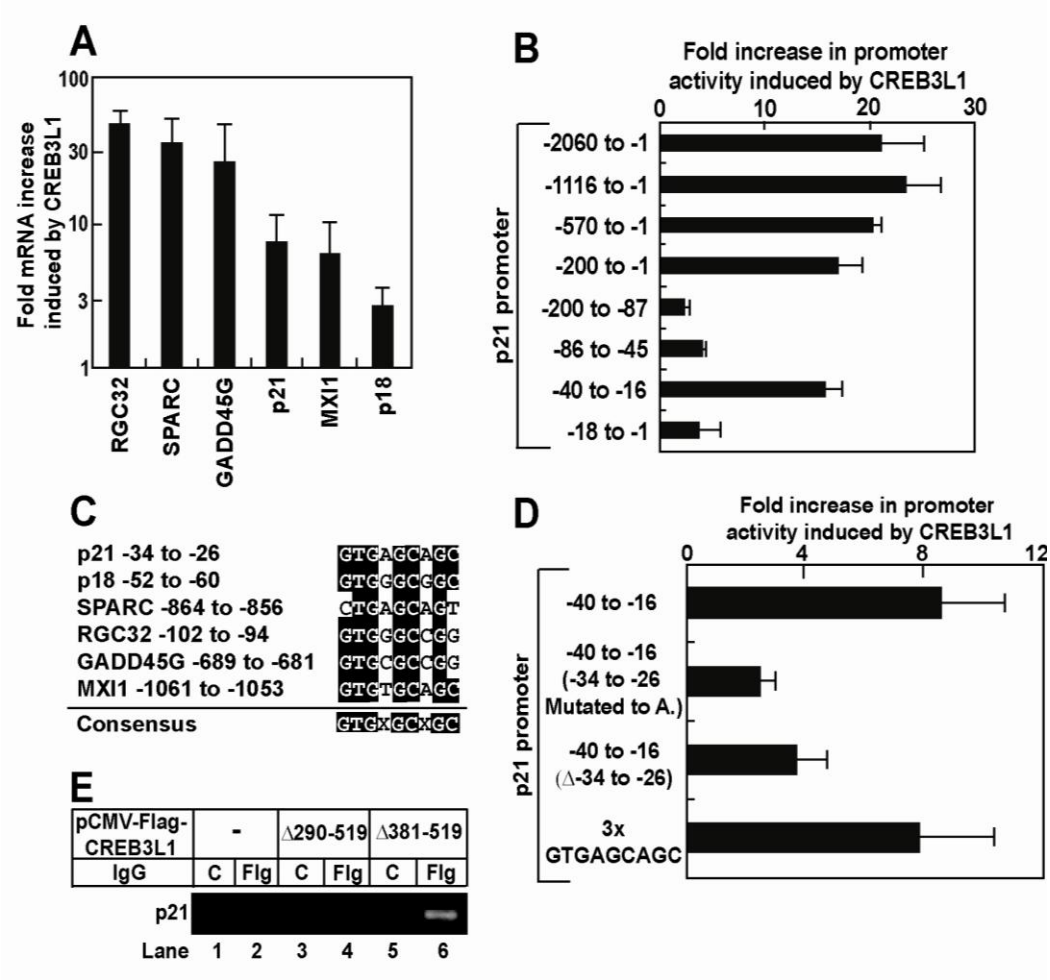

Figure 9. Nuclear Form of CREB3L1 Activates Genes that Inhibit the Cell Cycle
(A) Huh7-K2040 cells were seeded, transfected with pTracer or pTracer-CREB3L1(D381–519) as described in Figure 2D. The transfected cells were isolated based on GFP expression as described in Figure 2D. The amount of indicated mRNA was quantified by real-time QPCR. Fold induction of indicated mRNA by CREB3L1(D381–519) was determined by setting the amount of the mRNA in cells transfected with the control plasmid pTracer at 1. Results are reported as mean ± SD (n = 3).
(B and D) On day zero, Huh7-K2040 cells were seed at 7 x 10^5/60 mm dish. On day one, the cells were transfected with a firefly luciferase reporter plasmid containing the indicated region of p21 promoter (1 μg/dish) and a plasmid encoding Renilla luciferase driven by the constitutive CMV promoter (0.5 μg/dish) in the absence or presence of cotransfection of pCMV-CREB3L1(D381–519) (0.5 μg/dish). On day two, luciferase activity was measured, and the promoter activity was determined by firefly luciferase activity normalized against Renilla luciferase activity to control for transfection

efficiency. Fold increase in the promoter activity in cells transfected with CREB3L1(D381–519) compared to those mock transfected was presented. Results are reported as mean ± SD (n = 3).
(C) Alignment of -34 to -26 of the p21 promoter region with promoter sequences from indicated genes.

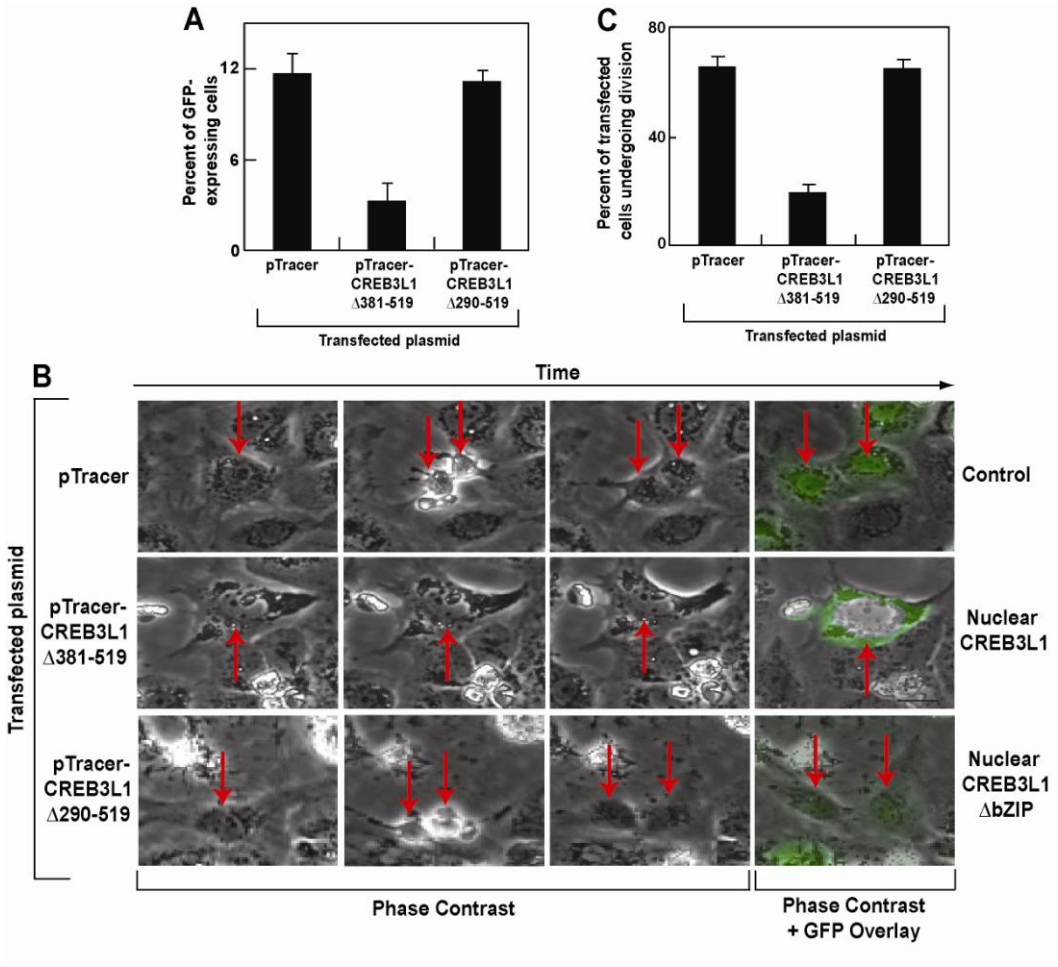

Figure 10. Nuclear Form of CREB3L1 Inhibits Cell Proliferation

(A) Huh7-K2040 cells were seeded and transfected with the indicated plasmid as described in Figure 2D. Three days after the transfection, percentage of the cells expressing GFP encoded by the transfected plasmid was determined through FACS analysis. Results are reported as mean ± SD (n = 3).

(B) On day zero, Huh7-K2040 cells were seeded at 2.5 x 10^5 per well of a 6-well plate. On day one, they were transfected with 0.25 μg of the indicated plasmid. On day two, the cells were subjected to time-lapse imaging analysis as described in Experimental Procedures. On day four (48 hr later), GFP fluorescence images were taken. Representative time-lapse images of these cells were shown, with arrows indicating transfected cells and their daughter cells determined by their expression of GFP at the end of the imaging at 48 hr.

(C) Quantification of transfected cells that went through cell divisions in (B). On average, 30 cells transfected with each plasmid were counted in each experiment. Results are reported as mean ± SD (n = 3).

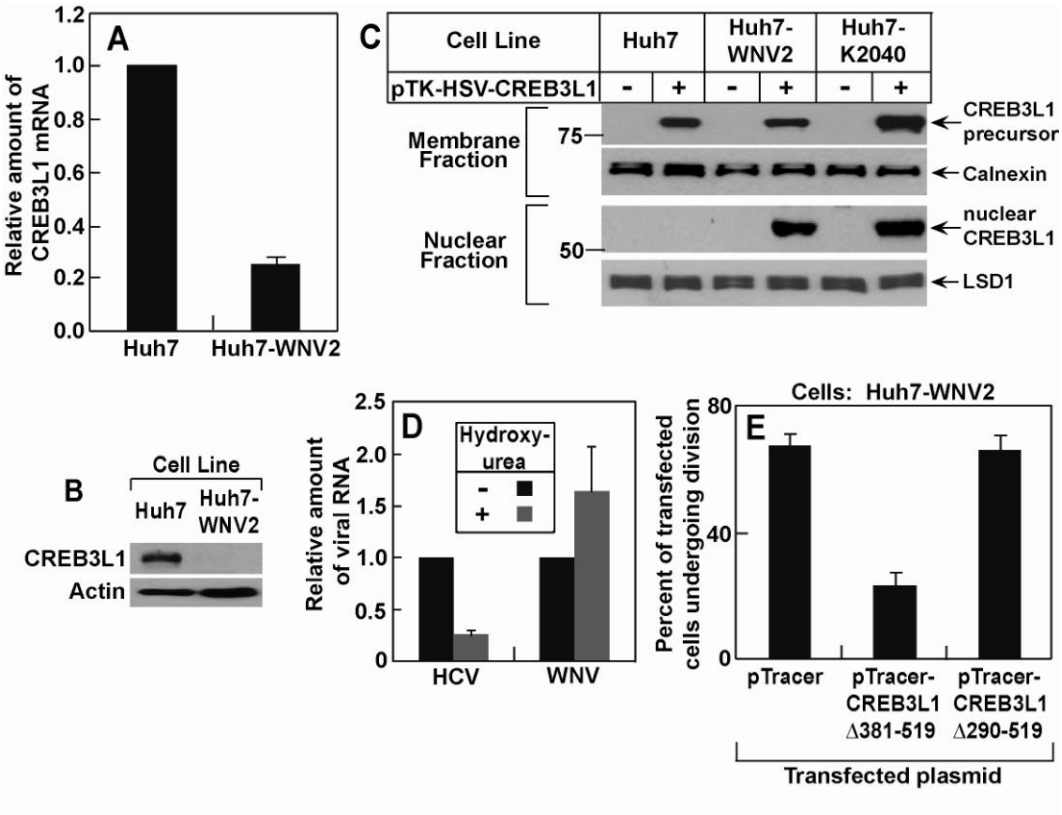

Figure 11. RIP of CREB3L1 Inhibits Proliferation of Cells Infected by WNV
(A) Real-time QPCR quantification of CREB3L1 mRNA in indicated cells with the value in Huh7 cells set to 1. Results are reported as mean ± SD (n = 3).
(B) Immunoblot analysis of CREB3L1 protein precursor in indicated cells is shown.
(C) Proteolytic cleavage of CREB3L1 was analyzed as described in Figure 5B.
(D) On day zero, Huh7-K2040 and Huh7-WNV2 cells were seeded at 2 3 105/60 mm dish. On day one, the cells were treated with or without 10 mM hydroxyurea. On day five, cells were harvested for quantification of HCV and WNV RNA in Huh7-K2040 and Huh7-WNV2 cells, respectively, by real-time QPCR, with the values in cells that were not treated with the drug set to 1. Results are reported as mean ± SD (n = 3).
(E) Quantification of Huh7-WNV2 cells transfected with indicated plasmid that went through cell divisions was carried out as described in Figure 8C.

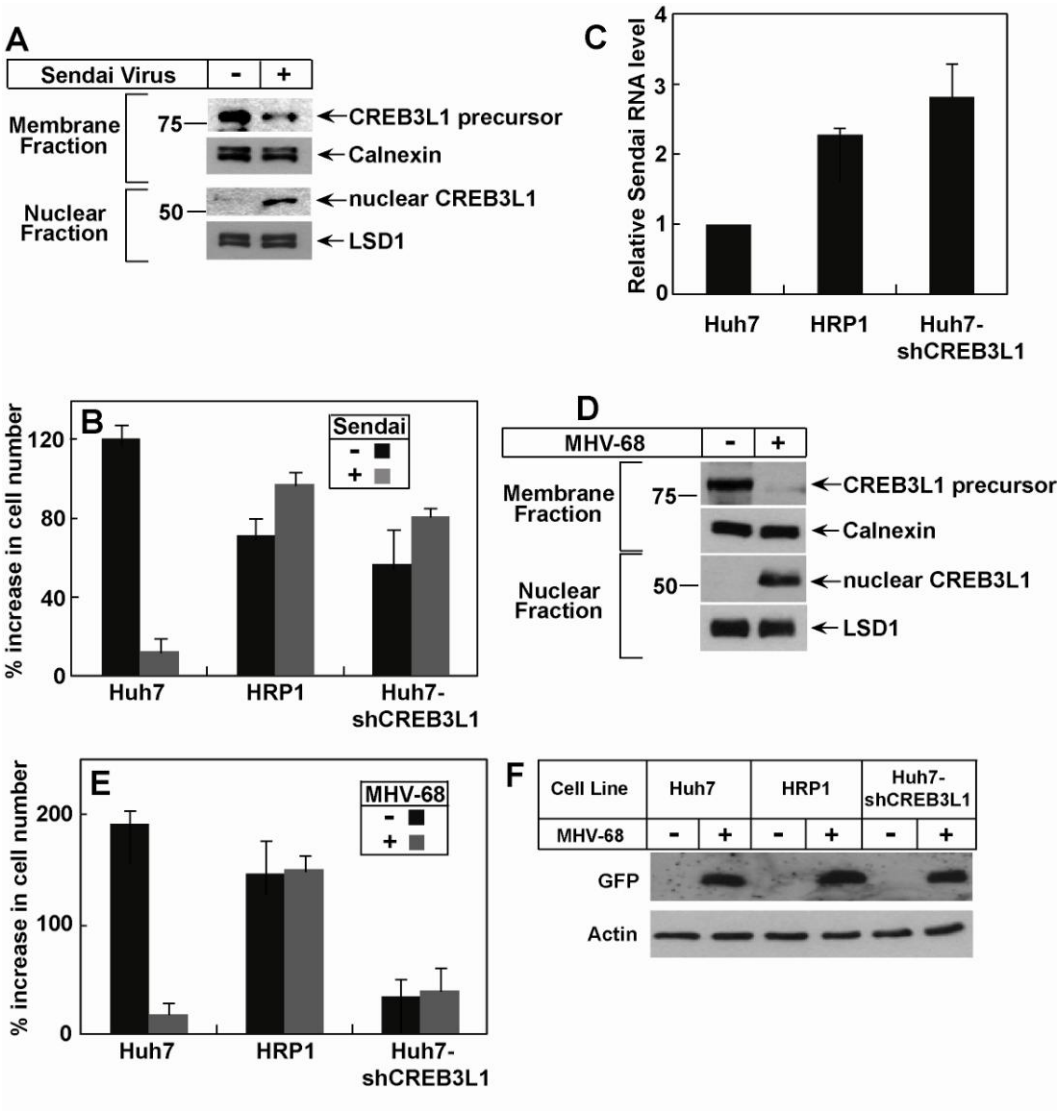

Figure 12. CREB3L1 Prevents Proliferation of Cells Infected by Sendai Virus and MHV-68

(A) On day zero, Huh7 cells were seeded at 4 x 10^5/60 mm dish. On day one, the cells were infected with Sendai virus. On day two, the cells were fractionated into nuclear and membrane fractions, and the cleavage of CREB3L1 was determined by immunoblot analysis with anti-CREB3L1. (All panels) Bar graphs are reported as mean ± SD (n = 3). **(B and C)** On day zero, Huh7, HRP-1, and Huh7- shCREB3L1 cells were seeded at 2 x 10^5/60 mm dish. On day one, triplicate dishes of the cells were harvested for cell counting. The remaining cells were infected with Sendai virus as indicated. On day two (24 hr later), triplicate dishes of these cells were harvested and the number of cells in each plate was quantified. The percentage increase in cell number on day two versus that

on day one is presented (B). Sendai virus RNA in the cells infected by the virus was quantified by real-time QPCR with the value in Huh7 cells set to 1 (C).
(D) Proteolytic cleavage of CREB3L1 was analyzed as in (A), except that the cells were infected by MHV-68 instead of Sendai virus.
(E and F) Indicated cells were seeded and treated as described in (B), except that the cells were infected by MHV-68 instead of Sendai virus. Proliferation of the cells was determined as described in (B). Cellular lysate was subjected to immunoblot analysis with anti-GFP (F).

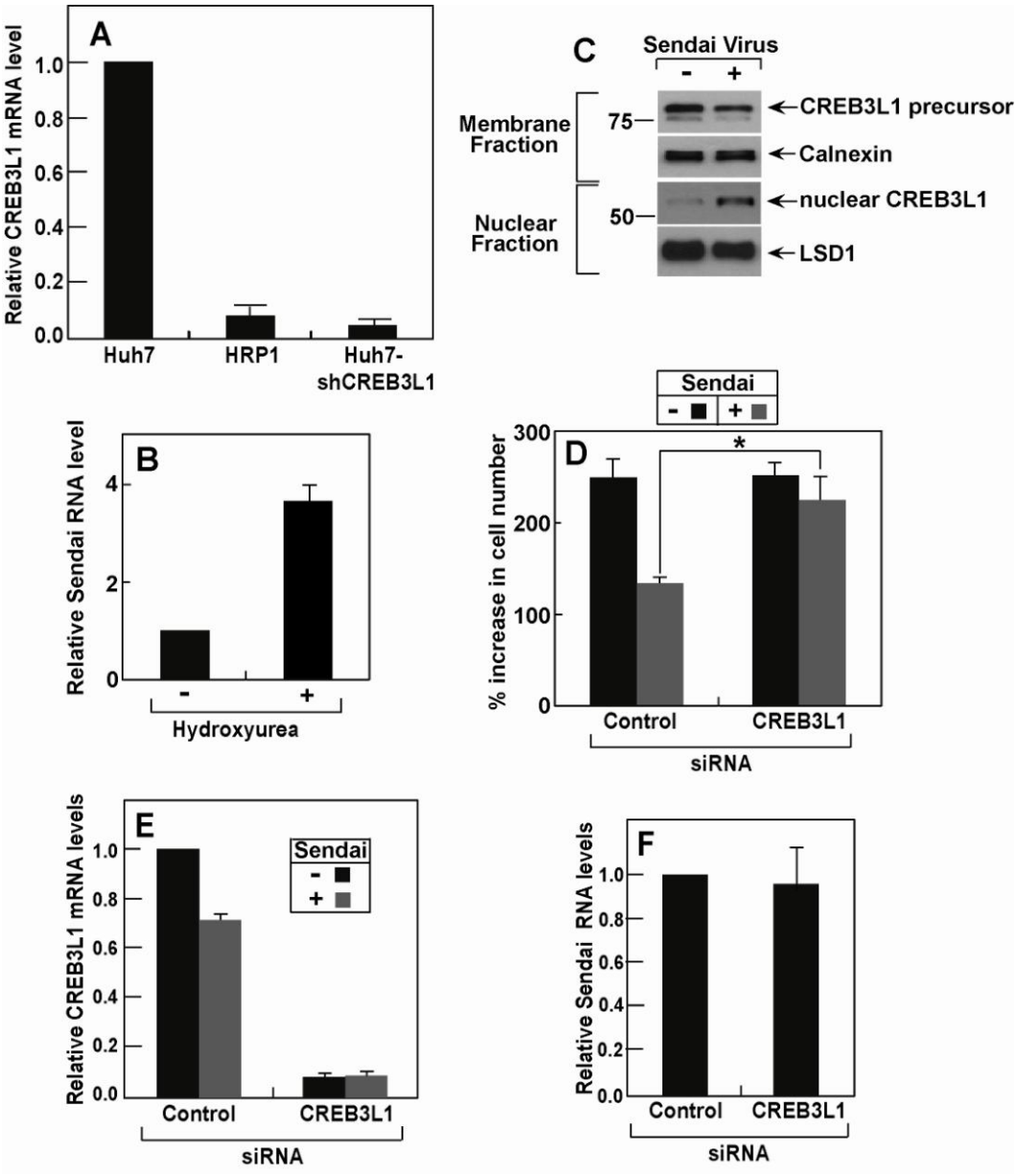

Figure 13. CREB3L1 Blocks Proliferation of Virus-Infected Cells
(A) RT-QPCR quantification of CREB3L1 mRNA in indicated cells with the value in Huh7 cells set to 1.
(B) On day 0 Huh7 cells were seeded at 2×10^5/60 mm dish. On day 1 they were infected by Sendai virus. On day 2, the cells were treated with 10 μM hydroxyurea as indicated. On day 4, the cells were harvested and the amount of Sendai virus RNA was quantified by RT-QPCR as described in Figure 5D.

(C) On day 0, SV589 cells were seeded at 4×10^5/60 mm dish. On day 1, the cells were infected with Sendai virus. On day 2, the cells were fractionated into nuclear and membrane fractions and the cleavage of CREB3L1 was determined by immunoblot analysis with anti-CREB3L1.
(D–F) On day 0, SV589 cells were seeded at 1×10^5/60 mm dish. On day 1, the cells were transfected with the indicated siRNA. On day 2, the cells were infected with Sendai virus. On day 3, the cells were harvested. Cell proliferation was determined as described in Figure 8B (D). *, $p < 0.01$. The amount of CREB3L1 mRNA was determined by RT-QPCR with the value in uninfected cells transfected with the control siRNA set to 1 (E). The amount of Sendai virus RNA in virus infected cells was quantified by RT-QPCR with the value in cells transfected with the control siRNA set to 1 (F). Bar graphs are reported as mean ± S.D. (n=3).

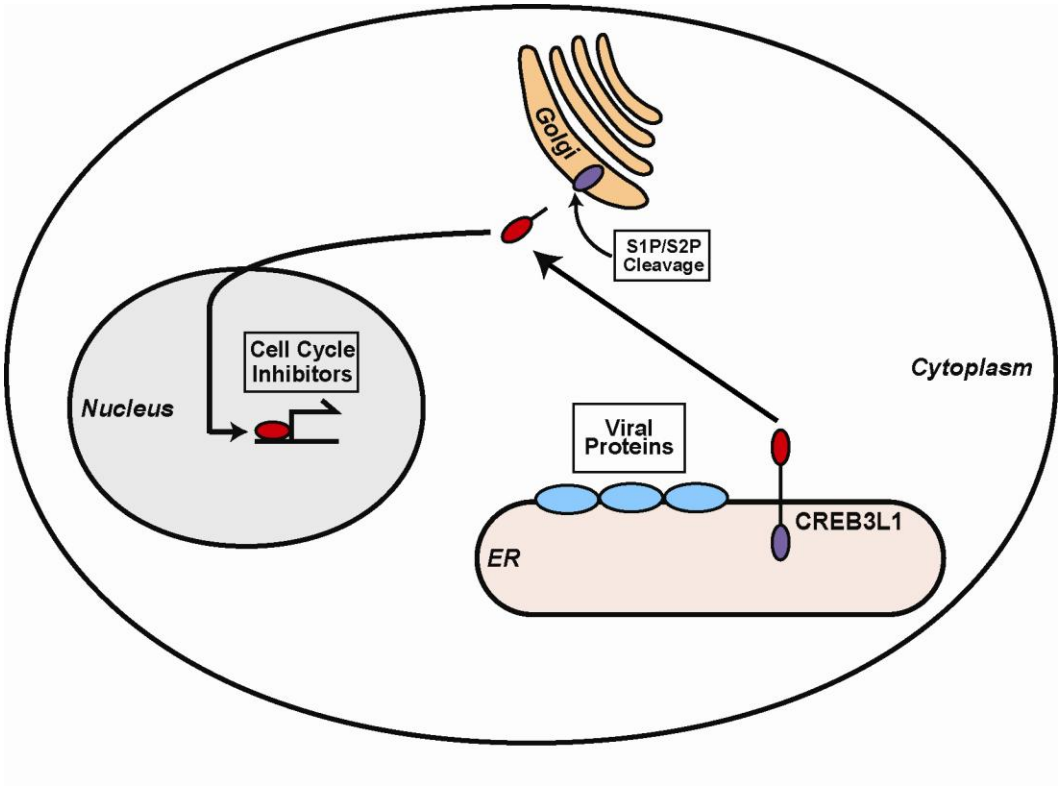

Figure 14. A Model Illustrating the Role of CREB3L1 in Limiting Proliferation of Virus-Infected Cells

CREB3L1 is synthesized as a membrane-bound precursor. In cells infected by virus, CREB3L1 is activated through RIP, presumably through ER stress caused by expression of ER-associated viral proteins. The proteolytic cleavage allows the NH2-terminal domain of the protein to enter the nucleus, where it activates transcription of genes encoding cell-cycle inhibitors to block proliferation of the cells infected by the virus.

Chapter 3: Doxorubicin blocks proliferation of cancer cells through proteolytic activation of CREB3L1

INTRODUCTION

Doxorubicin (Adriamycin®) is used widely to treat diverse types of cancer, yet its effectiveness is hampered by the existence of drug-resistant cancer cells. The reason for drug resistance is unclear mainly because the mechanism through which doxorubicin inhibits proliferation of cancer cells is not completely understood. Doxorubicin has been proposed to exert its cytostatic action through intercalation into DNA and production of free radicals (Gewirtz, 1999). However, these mechanisms are unlikely to be clinically relevant as the concentration of doxorubicin required to produce these effects is much higher than that achievable in patients (Gewirtz, 1999). Inhibition of topoisomerase II by doxorubicin at clinically achievable concentrations leads to DNA breaks, but a consistent relationship between DNA strand breaks and the cytostatic action of the drug has not been demonstrated (Gewirtz, 1999). Thus, the mechanism through which doxorubicin inhibits cell proliferation remains unclear.

In addition to blocking cell proliferation, doxorubicin induces renal fibrosis in mice by stimulating production of collagen (Lee and Harris, 2011). The dual ability of doxorubicin to block cell proliferation and to induce collagen expression caught our attention inasmuch as we recently showed that both responses can be activated by a transcription factor called cAMP response element-binding protein 3-like 1 (CREB3L1,

also known as OASIS) (Denard et al., 2011). These dual activities prompted us to hypothesize that doxorubicin functions by stimulating proteolytic activation of CREB3L1.

Here we report that doxorubicin functions by activating CREB3L1, a transcription factor synthesized as a membrane-bound precursor. Doxorubicin stimulates proteolytic cleavage of CREB3L1 by Site-1 Protease and Site-2 Protease, allowing the NH_2-terminal domain of CREB3L1 to enter the nucleus where it activates transcription of genes encoding inhibitors of the cell cycle, including *p21*. Knockdown of CREB3L1 mRNA in human hepatoma Huh7 cells conferred increased resistance to doxorubicin, whereas overexpression of CREB3L1 in human breast cancer MCF-7 cells markedly enhanced the sensitivity of these cells to doxorubicin. These results suggest that measurement of CREB3L1 expression may be a useful biomarker in identifying cancer cells sensitive to doxorubicin.

RESULTS

Doxorubicin triggers the Regulated Intramembrane Proteolysis of CREB3L1

To test whether doxorubicin activates cleavage of CREB3L1, we fractionated human hepatoma Huh7 cells (Nakabayashi et al., 1982) into membrane and nuclear fractions, and used an antibody reacting against the NH_2-terminal domain of CREB3L1 (Denard et al., 2011) to examine the cleavage of CREB3L1 through immunoblot analysis. In the absence of doxorubicin, CREB3L1 existed as the full length precursor (~ 80 kDa) in membranes and the cleaved nuclear form of CREB3L1 (~ 55 kDa) was barely detectable (Fig. 15B, lane 1). Treatment with doxorubicin markedly raised the amount of the nuclear form of CREB3L1 (Fig. 15B, lane 2). The amount of membrane protein

calnexin and nuclear protein lysine-specific demethylase 1 (LSD1) was not altered by doxorubicin treatment (Fig. 15A). To determine whether doxorubicin-stimulated cleavage of CREB3L1 was catalyzed by S1P and S2P, we analyzed the cleavage in mutant Chinese Hamster Ovary (CHO) cells deficient in S1P or S2P (Rawson et al., 1998; Rawson et al., 1997). In wild type CHO cells, doxorubicin stimulated cleavage of CREB3L1 to produce the nuclear form (Fig. 15C, lane 2). In contrast, doxorubicin failed to produce the nuclear form of CREB3L1 in mutant cells deficient in either S1P or S2P (Fig. 15C, lanes 4 and 6). In wild type CHO cells, we also detected in the membrane fraction a cleaved fragment with a molecular weight similar to that of the nuclear form (Fig. 15C, lanes 1-2). This fragment was absent in cells deficient in S1P (Fig. 15C, lanes 3-4) but dramatically elevated in cells deficient in S2P (Fig. 15C, lanes 5-6). These findings suggest that this membrane-bound fragment is the intermediate form of CREB3L1 that was cleaved by S1P but not by S2P. Similar cleavage intermediates were observed in earlier studies of SREBP-2 and ATF6, two prototypes of RIP substrates, in mutant CHO cells deficient in S2P (Rawson et al., 1997; Ye et al., 2000b).

Doxorubicin triggers transcription of CREB3L1 target genes and blocks cell proliferation

In Huh7 cells transfected with a control shRNA (Huh7-shControl), doxorubicin induced the expression of *collagen 1α1* and *p21* (Figs. 16A and 16B), both of which were shown to be direct targets of CREB3L1 (Denard et al., 2011; Murakami et al., 2009) (Figs. 16A and 16B). In Huh7 cells stably transfected with a shRNA targeting CREB3L1 (Huh7-shCREB3L1) in which expression of CREB3L1 was drastically reduced (Fig. 17A)

(Denard et al., 2011), induction of these genes was markedly blunted (Figs. 16A, 16B, 17B and 17C). Since CREB3L1 was required for doxorubicin to induce expression of *p21*, a well-characterized inhibitor of the cell cycle(Sherr and Roberts, 1999), we determined whether CREB3L1 was also required for the drug to inhibit cell proliferation. For both untransfected Huh7 cells and those transfected with the control shRNA (Huh7-shControl), doxorubicin completely blocked their proliferation at a concentration between 50 and 150 nM (Fig. 16C), which was also the concentration that resulted in maximal cleavage of CREB3L1 (Fig. 16D). For Huh7-shCREB3L1 cells, doxorubicin at concentrations up to 500 nM failed to block their proliferation (Fig. 16C). These concentrations of doxorubicin were not enough to trigger apoptosis of Huh7 cells, which became apparent only when the cells were treated with 5 μM of the compound (Fig. 16E).

CREB3L1 expression levels correlate with sensitivity to doxorubicin

If proteolytic activation of CREB3L1 is required for doxorubicin to inhibit cell proliferation, then the amount of CREB3L1 expressed in cancer cells may determine their sensitivity to doxorubicin. To test this hypothesis, we analyzed SV589 cells, an immortalized line of human fibroblasts (Yamamoto et al., 1984), and MCF-7 cells, a line of human breast cancer cells (Soule et al., 1973). Compared to Huh7 cells, expression of CREB3L1 was higher in SV589 cells and lower in MCF-7 cells (Fig. 18A). The sensitivity of the cells to growth inhibition by doxorubicin followed the order of CREB3L1 expression (Fig. 18B). Similar to Huh7 cells, knockdown of CREB3L1 by two duplexes of siRNA targeting different regions of CREB3L1 in SV589 cells (Fig. 19A) made them more resistant to doxorubicin (Fig, 18C). Since MCF-7 cells expressed very

little CREB3L1, we used these cells to study the effect of CREB3L1 overexpression on sensitivity to doxorubicin. We stably transfected MCF-7 cells with a plasmid encoding CREB3L1 and selected one clone of the cells with relatively low expression (MCF7/pCREB3L1(L); 8-fold above parental cells) and another clone with high expression of CREB3L1 (MCF7/pCREB3L1(H); 300-fold above parental cells) (Fig. 18D). The 8-fold overexpression of CREB3L1 in MCF7/pCREB3L1(L) cells lowered the IC_{50} for doxorubicin from 500 nM to 10 nM, and the 300-fold overexpression of CREB3L1 in MCF7/pCREB3L1(H) cells further reduced the IC_{50} to ~1 nM (Fig. 18E). In this experiment, cells were treated with doxorubicin for 2 days. To determine the effect of CREB3L1 expression on proliferation of the cells treated with doxorubicin for a longer period of time, we incubated MCF-7 and MCF7/pCREB3L1(H) cells with 15 nM doxorubicin for 6 days. This treatment did not affect proliferation of MCF-7 cells, but markedly blocked proliferation of MCF7/pCREB3L1(H) cells, as determined by direct cell counting (Fig. 18F) and by measurement of cellular DNA content (Fig. 19B). Thus, CREB3L1 expression level is a key determinant of cellular sensitivity to doxorubicin.

CREB3L1 activation is independent from DNA damage

We then determined the relationship between doxorubicin-induced cleavage of CREB3L1 and DNA breaks caused by inhibition of topoisomerase. Doxorubicin induced appearance of histone γH2AX, a marker for DNA breaks (Fig. 20A, lane 2). However, this effect was unaffected by knockdown of CREB3L1 expression (Fig. 20A, lane 5). This result suggests that cleavage of CREB3L1 does not lead to doxorubicin-induced DNA breaks. To investigate whether DNA breaks may lead to cleavage of CREB3L1, we

examined etoposide, another chemotherapeutic drug that inhibits topoisomerase (Stahelin and von Wartburg, 1991). Unlike doxorubicin, eptoposide failed to induce cleavage of CREB3L1 (Fig. 20B, lane 3), even though the compound was as effective as doxorubicin in causing DNA breaks (Fig. 20A, lanes 2 and 3). Accordingly, knockdown of CREB3L1 in Huh7 cells did not increase their resistance to etoposide (Fig. 20C), and overexpression of CREB3L1 in MCF7 cells also did not increase their sensitivity to the compound (Fig. 20D). These results suggest that induction of CREB3L1 cleavage by doxorubicin is not related to its activity of topoisomerase inhibition. Besides etoposide, CREB3L1 is also not required for bleomycin or paclitaxel to inhibit cell growth, an observation suggesting that CREB3L1 may be specifically involved in doxorubicin-induced suppression of cell proliferation (Figs. 20E-G).

Doxorubicin-induced synthesis of ceramide stimulates cleavage of CREB3L1

RIP of membrane-bound transcription factors is known to be a signal transduction pathway that transfers signals from the ER to nucleus (Brown et al., 2000). Since ER is the site for synthesis of most lipids, we wondered whether doxorubicin may alter homeostasis of certain lipids that may result in cleavage of CREB3L1. Daunorubicin, a chemotherapeutic drug derived from doxorubicin, was reported to induce *de novo* synthesis of ceramide (Bose et al., 1995). We determined that doxorubicin also stimulated ceramide synthesis by showing that treatment with the compound increased the amount of tritium-labeled palmitate incorporated into ceramide in Huh7 cells (Fig. 21A). Myriocin, an inhibitor of ceramide synthesis (Miyake et al., 1995), inhibited doxorubicin-induced cleavage of CREB3L1 in a dose-dependent manner (Fig. 21B,

lanes 5-8). Co-treatment with myriocin also rendered the cells more resistant to doxorubicin (Fig. 21C). Exogenously added C_6-ceramide, a cell-permeable analogue of ceramide that contains a short acyl chain (C_6-ceramide), stimulated CREB3L1 cleavage even in the absence of doxorubicin (Fig. 21D). These results suggest that doxorubicin-induced synthesis of ceramide leads to cleavage of CREB3L1. Thus, CREB3L1 appears to suppress cell proliferation in response to accumulation of ceramide. This conclusion was further supported by the observation that knockdown of CREB3L1 in Huh7 cells completely abolished the ability of C_6-ceramide to inhibit cell proliferation (Fig. 21E).

DISCUSSION

The current study establishes a crucial role for CREB3L1 in mediating inhibition of cell proliferation in response to doxorubicin. The concentration of doxorubicin required to proteolytically activate CREB3L1 is within the range of concentrations in serum of patients treated with doxorubicin ($< 1\ \mu M$) (Gewirtz, 1999). These findings raise the possibility that the clinical response to doxorubicin may be determined by the level of CREB3L1 produced in tumor cells. Thus, measuring CREB3L1 expression in tumor cells may be useful in identifying cancer patients who are most likely to benefit from doxorubicin treatment.

Topoisomerase inhibition and subsequent DNA damage has long thought to be the mechanism though which doxorubicin prevents cell proliferation. The data presented here point to DNA damage as a harmful side effect rather than therapeutic as DNA damage occurs in the absence of the anti-proliferative effect in CREB3L1-deficient cells. It is possible that doxorubicin-induced DNA damage could stimulate healthy patient cells

to become cancerous though DNA damage. This data suggests the need for new drugs than specifically target CREB3L1.

The fact that myriocin treatment and addition of exogenous ceramide trigger CREB3L1 cleavage and subsequent cessation of cell proliferation provide some evidence that CREB3L1 is a ceramide sensor for the ER. The data also suggest ceramide is merely a signaling molecule due to the fact that it is not detrimental to CREB3L1-deficient cell proliferation. The proto-type membrane transcription factor , SREBP, requires adapter proteins that directly sense cholesterol. Perhaps CREB3L1 function in the same manner for sphingolipids. If this holds true, CREB3L1 may be important for other cellular functions yet to be recognized.

MATERIALS AND METHODS

Materials

We obtained rabbit anti-LSD1 from Cell Signaling; mouse anti-calnexin from Enzo Life Sciences; mouse anti-γH2AX from Millipore; rabbit anti-Actin from Abcam; peroxidase-conjugated secondary antibodies from Jackson ImmunoResearch; Doxorubicin (Cat# D1515-10MG), bleomycin, etoposide, paclitaxel and N-Hexanoyl-D-sphingosine (C_6-Ceramide) from Sigma-Aldrich; Myriocin from EMD Biosciences; and [^{3}H]palmitate from ARC. A rabbit polyclonal antibody against human CREB3L1 was generated as previously described (Denard et al., 2011). Doxorubicin stock solution (2.5 mg/ml) was made by adding nuclease-free water (Ambion) directly to the vial, and was stored at 4 °C for no more than 2 weeks.

Cell Culture

SRD-12B and M19 cells are mutant CHO cells deficient in S1P and S2P, respectively (Rawson et al., 1998; Rawson et al., 1997). These cells were maintained in medium A (1:1 mixture of Ham's F12 medium and Dulbecco's modified Eagle's medium containing 100 U/ml penicillin and 100 µg/ml streptomycin sulfate) supplemented with 5% (v/v) fetal calf serum (FCS), 5 µg/ml cholesterol, 1 mM sodium mevalonate, and 20 µM sodium oleate. Their parental CHO-7 cells are a clone of CHO-K1 cells selected for growth in lipoprotein-deficient serum (Metherall et al., 1989) and were maintained in medium A supplemented with 5% (v/v) newborn calf lipoprotein-deficient serum. Huh7 and SV589 cells were maintained in medium B (Dulbecco's modified Eagle's medium

with 4.5 g/l glucose, 100 U/ml penicillin, 100 mg/ml streptomycin sulfate, and 10% (v/v) FCS). Single cell clones of Huh7-shControl and Huh7-shCREB3L1 cells were generated by stably transfecting Huh7 cells with a control shRNA or shRNA targeting CREB3L1, respectively, as previously described (Denard et al., 2011). These cells were maintained in medium B supplemented with 10 µg/ml puromycin. MCF-7 cells were maintained in medium C (RPMI-40 media with 100 U/ml penicillin, 100 mg/ml streptomycin sulfate, and 10% (v/v) FCS). MCF7/pCREB3L1(L) and MCF7/pCREB3L1(H) were generated by stably transfecting MCF-7 cells with pTK-CREB3L1 encoding human CREB3L1 driven by the thymidine kinase promoter. These cells were maintained in medium C supplemented with 700 µg/ml G418. All cells were incubated in monolayers at 37 °C in 5% CO_2 except for CHO and MCF-7-derived cells that were cultured at 37 °C in 8% CO_2.

Immunoblot Analyses

Cell homogenates were separated into nuclear and membrane fractions (Sakai et al., 1996), and analyzed by SDS-PAGE (15% for γH2AX and 10% for the rest of the proteins) followed by immunoblot analysis with the indicated antibodies (1:1000 dilution for anti-CREB3L1 and anti-LSD1, 1:3000 dilution for anti-calnexin, 1:2000 dilution for anti-γH2AX and 1:10,000 dilution for anti-Actin) . Bound antibodies were visualized with a peroxidase-conjugated secondary antibody using the SuperSignal ECL-HRP substrate system (Pierce).

RT-QPCR

RT-QPCR was performed as previously described (Liang et al., 2002). Each measurement was made in triplicate from cell extracts pooled from duplicate dishes. The relative amounts of RNAs were calculated through the comparative cycle threshold method by using human 36B4 mRNA as the invariant control except for the results shown in Figs. 17B and 17C in which GAPDH mRNA served as the invariant control.

Cell Quantification

On day 0, cells were seeded at 1.5×10^5/60-mm dish. On day 1, the cells were treated with indicated concentration of doxorubicin. Following incubation for the indicated time, the number of cells was determined by direct counting or measurement of cellular DNA content with Quant-iT dsDNA Assay Kit (Life Technologies). Each measurement was reported as the mean value from triplicate incubations.

RNA Interference

Duplexes of siRNA were synthesized by Dharmacon Research. The siRNA sequences targeting human CREB3L1 and the control siRNA targeting GFP was reported previously (Adams et al., 2004; Denard et al., 2011). Cells were transfected with siRNA using Lipofectamine RNAiMAX reagent (Invitrogen) as described by the manufacturer, after which the cells were used for experiments as described in the figure legends.

TUNEL Assay

TUNEL assay was performed with the APO-BrdU TUNEL Assay kit (Invitrogen) as described in the manufacturer's directions. Cells were subjected to flow cytometry on a

FACSCaliber Flow Cytometer (Becton Dickinson) to determine percent of apoptotic cells. At least 5000 cells were collected for each measurement. Results from each experiment were reported as mean of triplicate measurements.

Measurement of Ceramide Synthesis

On day 0, Huh7 cells were seeded at 4×10^5/60-mm dish. On day 1, the cells were treated with or without 200 nM doxorubicin. On day 2, the cells were labeled with [^{3}H]palmitate as described in figure legend. Following homogenizing the cells in buffer A (10 mM HEPES pH 7.6, 1.5 mM $MgCl_2$, and 10 mM KCl), lipids in the homogenate were extracted by 0.5 ml of chloroform/methanol (2:1; v/v), dried, and dissolved in 70 µl of chloroform/methanol (1:1; v/v). Lipid extracts were mixed with 50 µg of non-radioactive ceramide standard (Avanti Polar Lipids) and analyzed by Thin Layer Chromotography (TLC) on POLYGRAM SIL G plates in a solvent system of chloroform/acetate (90:10; v/v) for ceramide separation. Following visualization by exposing the TLC plates to I_2 vapor, bands containing ceramide were excised, and the amount of radioactivity in it was determined by scintillation counting. The activity of ceramide synthesis was determined by radioactivity found in the ceramide band normalized by the amount of cellular protein.

Chapter 3 Figures

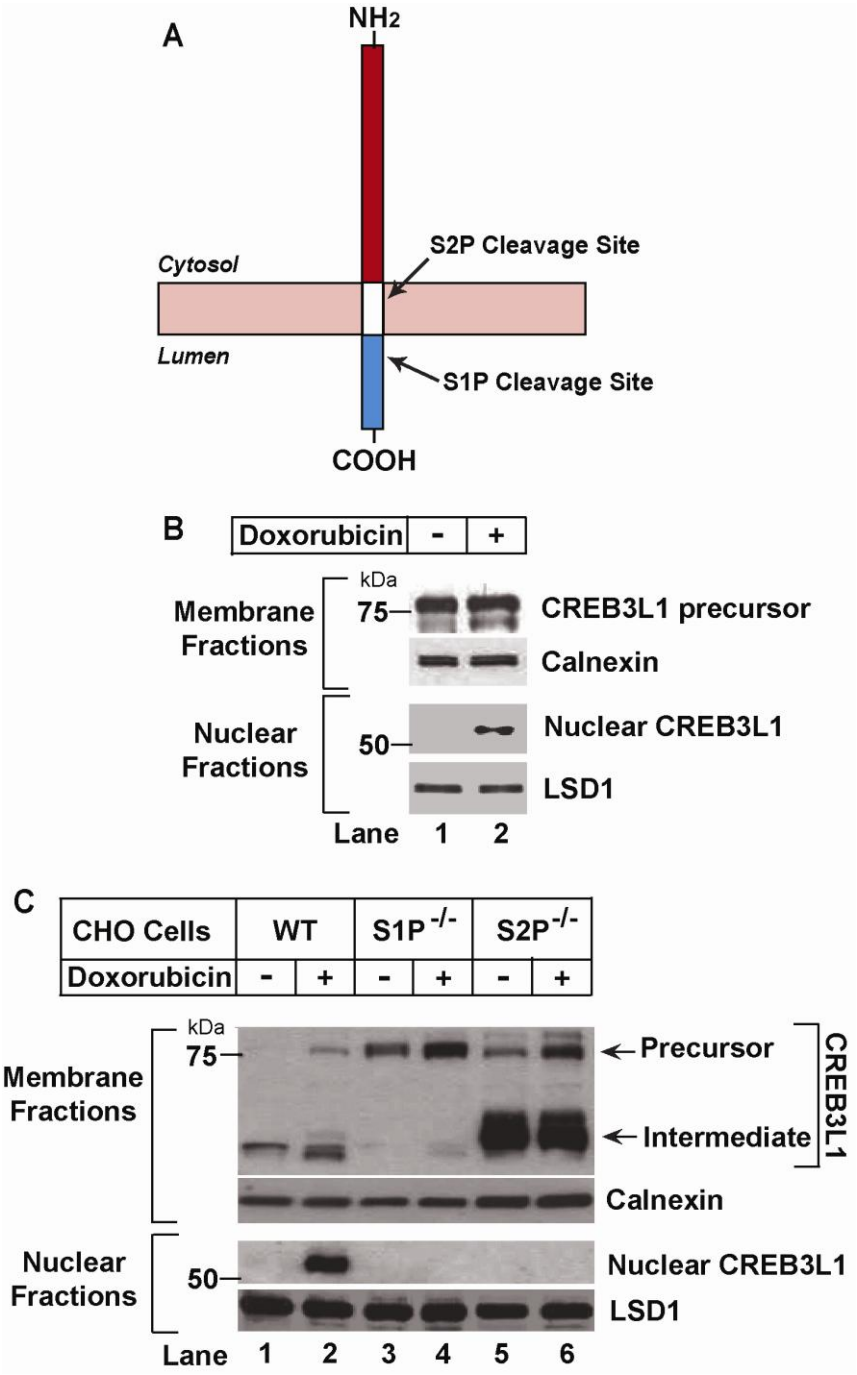

Figure 15. Doxorubicin stimulates RIP of CREB3L1

(**A**) Schematic diagram of CREB3L1.
(**B and C**) Huh7 cells (**B**) or wild type and mutant CHO cells (**C**) were treated with 500 nM doxorubicin for 24 h, separated into nuclear and membrane fractions, and analyzed by immunoblot with antibodies directed against CREB3L1, calnexin and LSD1. Similar results were observed in multiple independent experiments.

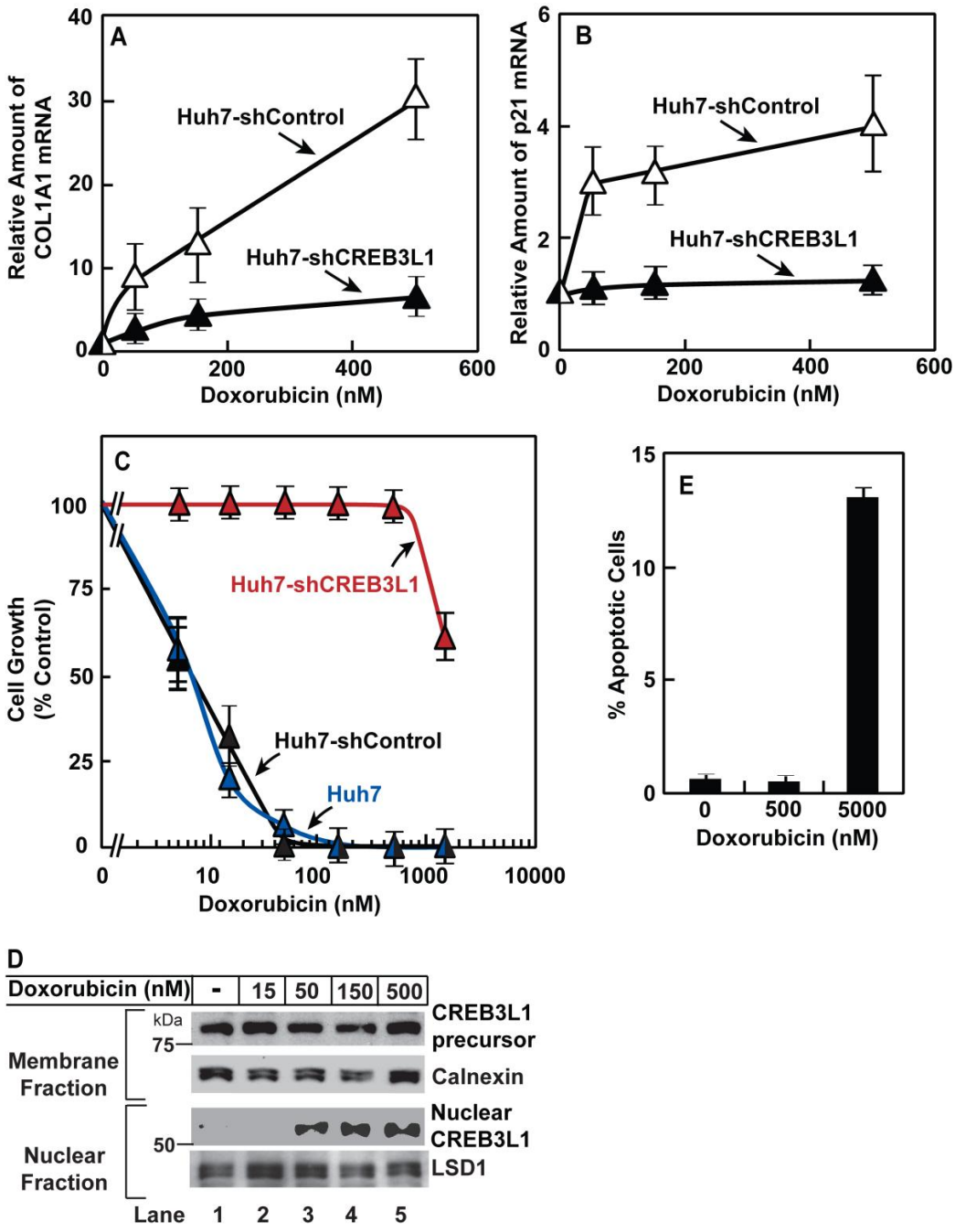

Figure 16. CREB3L1 is required for doxorubicin to inhibit proliferation of Huh7 cells

(**A** and **B**) Collagen 1α1 (COL1A1) (**A**) and p21 (**B**) mRNAs were quantified by RT-QPCR after the indicated cells were treated with the indicated concentration of doxorubicin for 72 h (**A**) or 24 h (**B**). The value of each mRNA in cells that were not treated with doxorubicin is set to 1. (**C**) Cell numbers were counted after the indicated cells were treated with the indicated concentration of doxorubicin for 48 h. The number of cells just prior to the drug treatment and after treatment with no drug for 48 h is set to 0% and 100%, respectively. (**D)** Huh7 cells were treated with the indicated concentrations of doxorubicin and analyzed as described in Fig. 1B. Similar results were observed in multiple independent experiments. (**E**) Huh7 cells were treated with the indicated concentrations of doxorubicin for 48 h before they were harvested for TUNEL assay to determine percentage of cells that underwent apoptosis. (**A**, B, **C** and **E)** Results are reported as mean ± S.E.M. of three independent experiments.

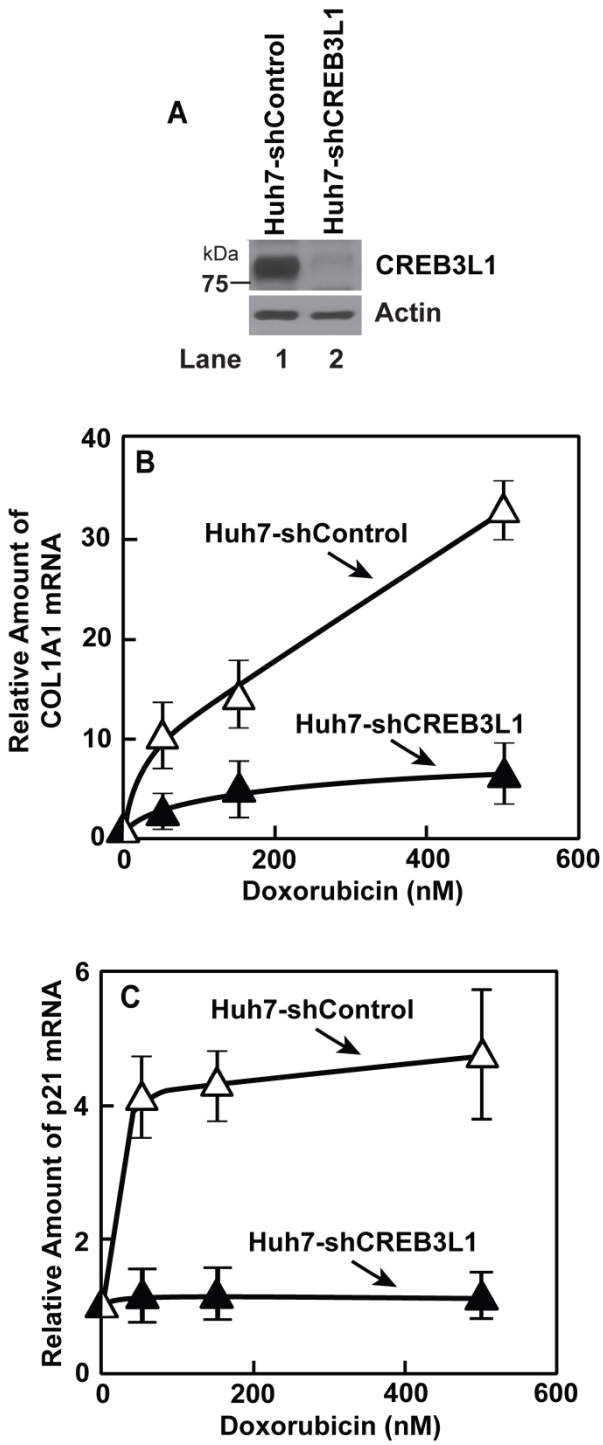

Figure 17. CREB3L1 is required for doxorubicin to suppress proliferation of Huh7 cells

(**A**) Immunoblot analysis of CREB3L1 in indicated cells. (**B** and **C**) RT-QPCR analyses were performed as described in Figs. 2A and 2B except that GADPH mRNA was used as the invariant control.

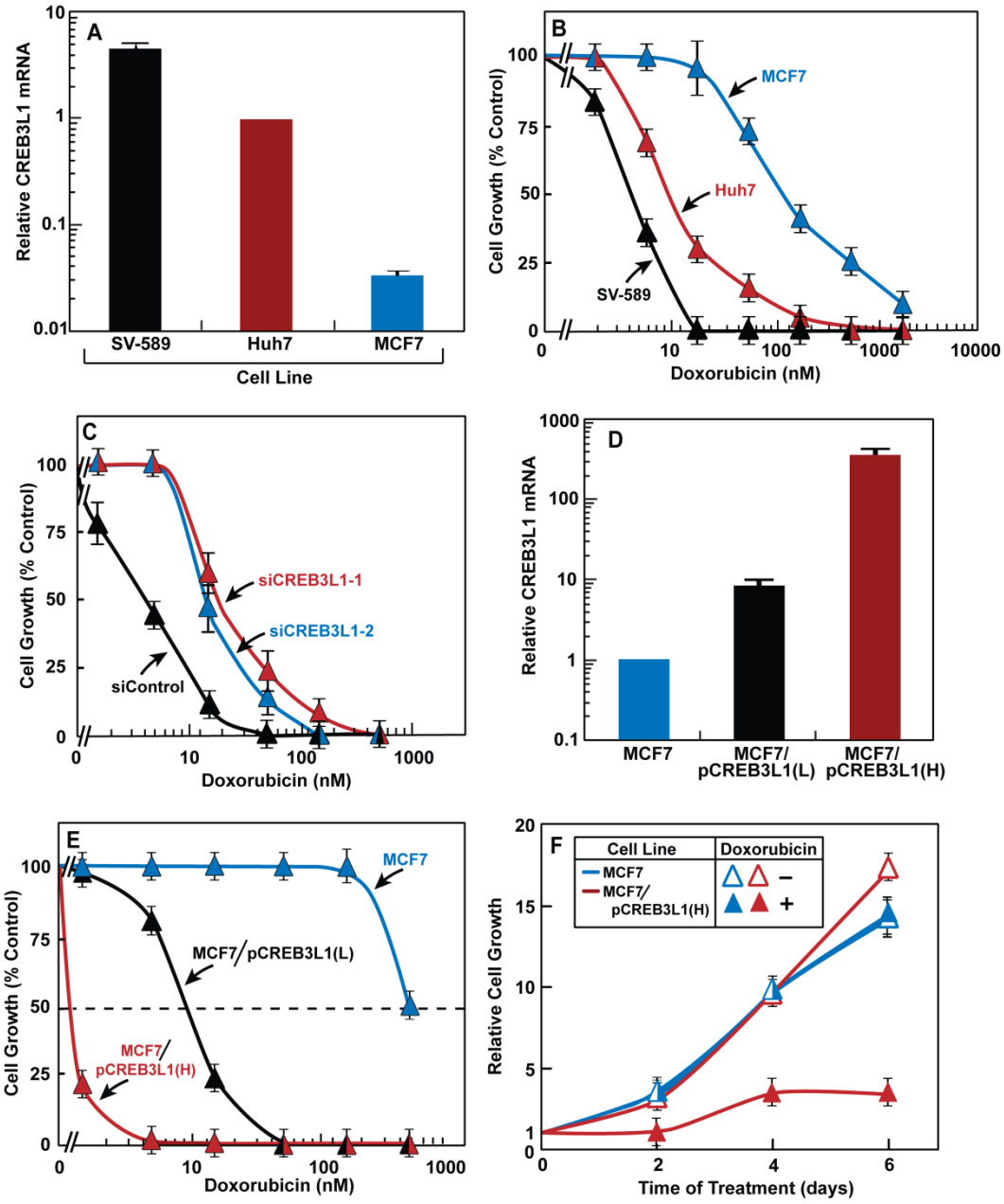

Figure 18. Sensitivity of cancer cells to doxorubicin is correlated with expression of CREB3L1

(**A** and **D**) RT-QPCR quantification of CREB3L1 mRNA in indicated cells with its value in Huh7 (**A**) or MCF-7 cells (**D**) set to 1. C_T values of CREB3L1 mRNA in SV589, Huh7 and MCF-7 cells were 20, 23, and 28, respectively. (**B** and **E**) Effect of doxorubicin on proliferation of the indicated cells was determined as described in Fig. 2C. (**C**) SV589

cells were transfected with indicated siRNA and their sensitivity to doxorubicin was analyzed as described in Fig. 2C. (**F)** Cell numbers were quantified after indicated cells were treated with or without 15 nM doxorubicin for the indicated period of time. The number of cells just before doxorubicin treatment at time 0 is set to 1. (**A**-**F**) Results are reported as mean ± S.E.M. of three independent experiments.

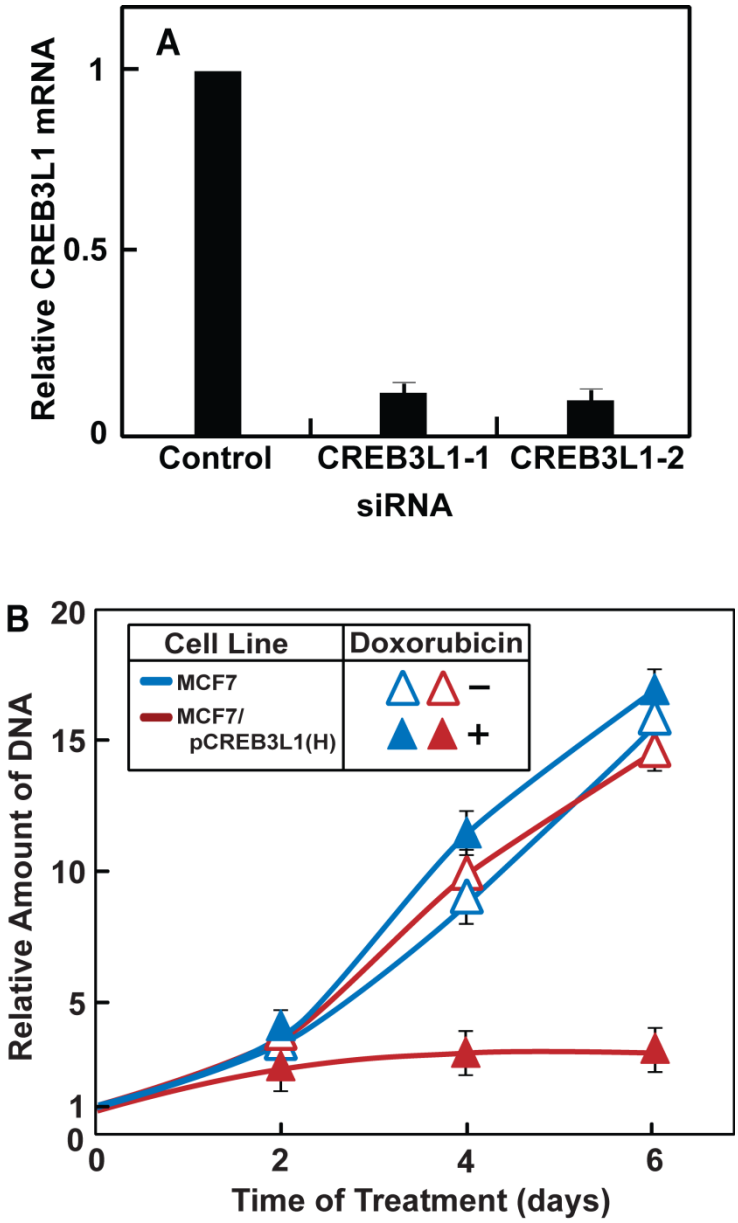

Figure 19. Sensitivity of cancer cells to doxorubicin is correlated to their expression of CREB3L1

(**A**) RT-QPCR analysis of CREB3L1 mRNA in SV589 cells transfected with indicated siRNA in experiments shown in Figure 3C. CREB3L1 mRNA level in cells transfected with control siRNA is set to 1. (**B**) Quantification of DNA in cells used in experiments shown in Fig. 3F. The amount of DNA in cells just prior to the drug treatment at time zero is set to 1. (**A** and **B**) Results are reported as mean ± S.E.M. from three independent experiments.

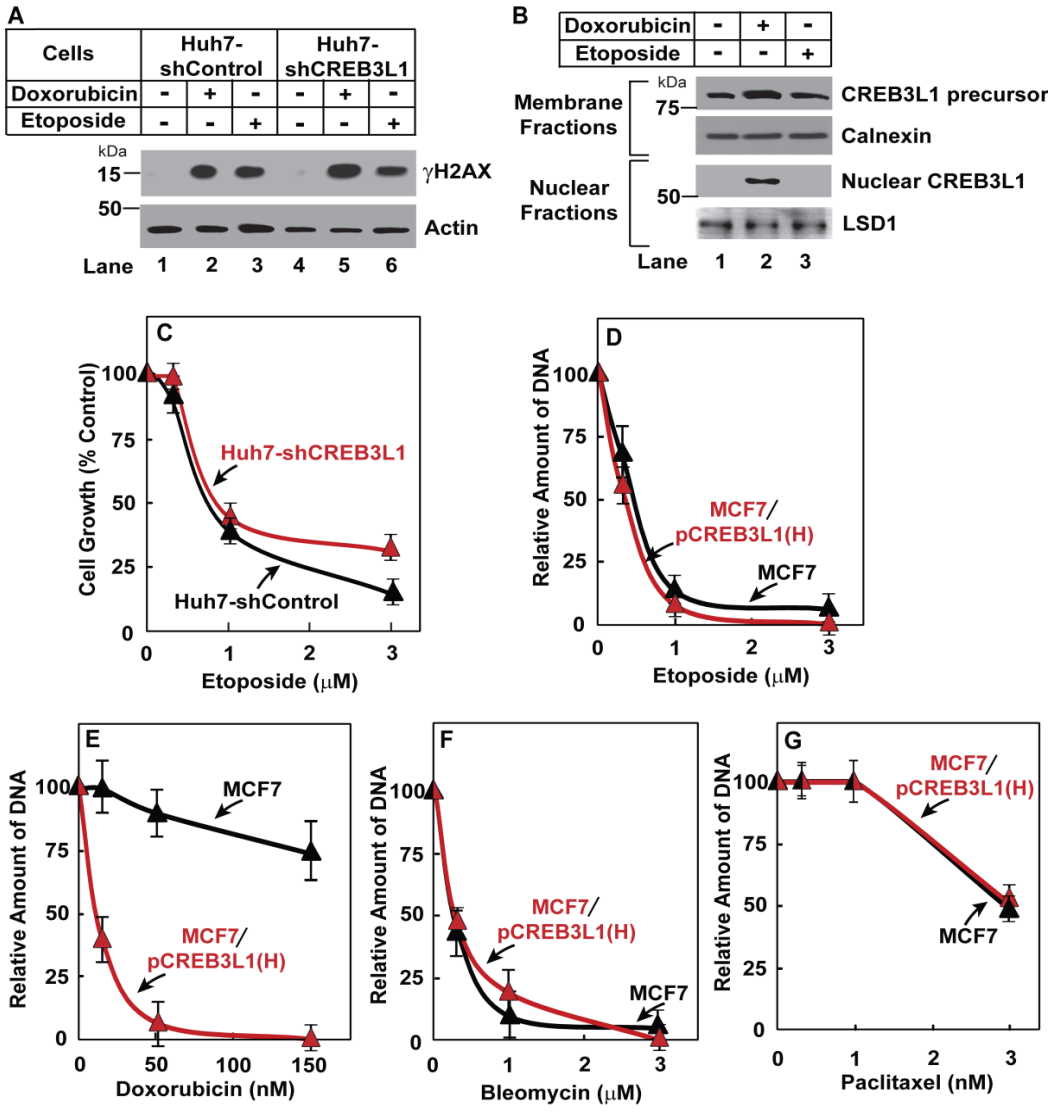

Figure 20. CREB3L1 activation is independent from DNA breaks
(A) Indicated cells were treated with 500 nM doxorubicin or 500 nM Etoposide for 24 h and harvested for immunoblot analysis of γH2AX with actin as a loading control. (**B**) Huh7 cells were treated with 500 nM doxorubicin or 500 nM etoposide for 24 h and analyzed as described in Fig. 1B. (**C**) The effect of etoposide on proliferation of the indicated cells was determined as described in Fig. 2C. (**D-G**) Indicated cells were treated with indicated concentrations of etoposide (**D**), doxorubicin (**E**), bleomycin (**F**), or paclitaxel (**G**) for 48 h before the cells were harvested for quantification of DNA to determine cell growth as described in Fig. S2B.

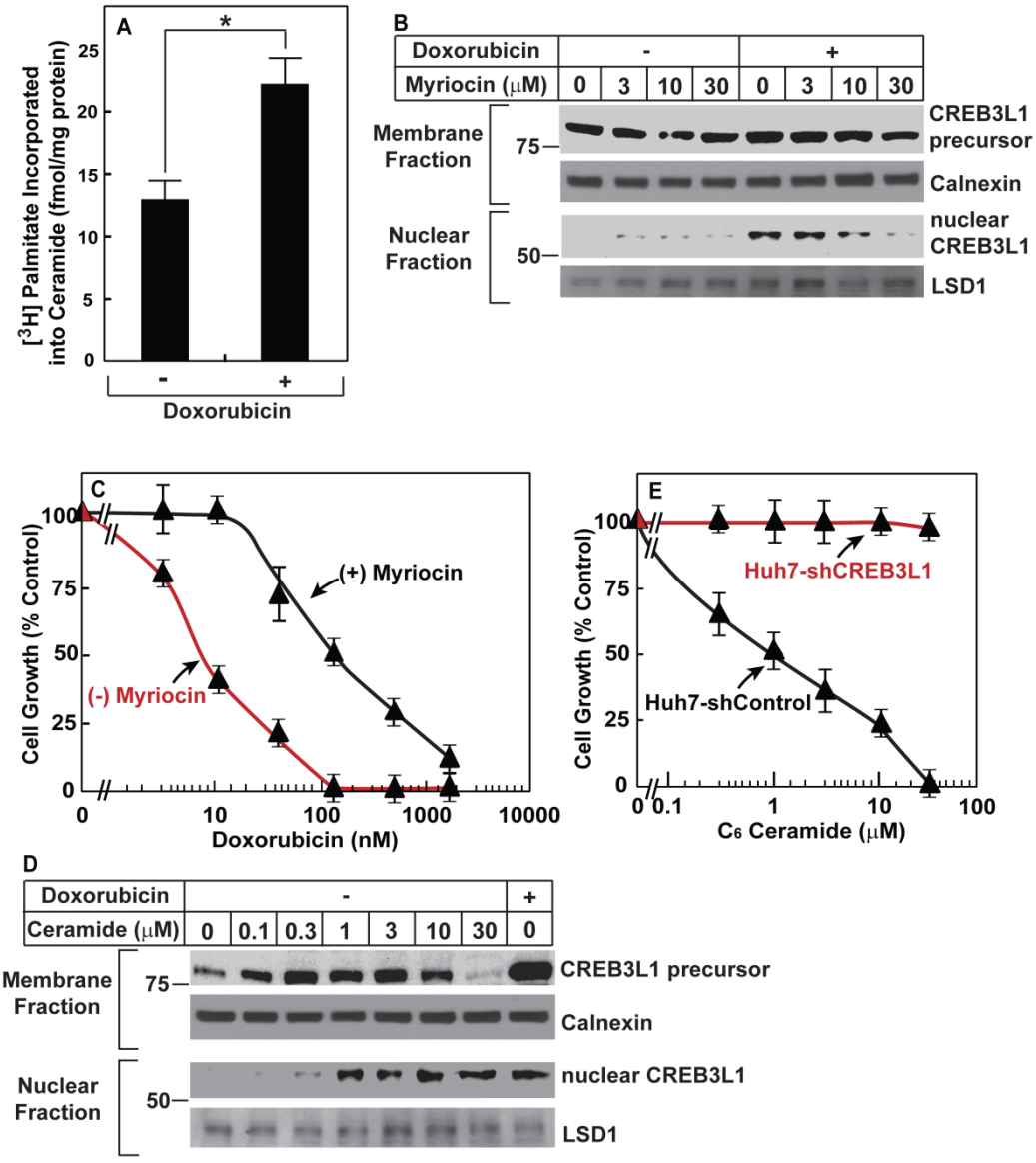

Figure 21. Doxorubicin-induced synthesis of ceramide stimulates cleavage of CREB3L1

(**A**) Huh7 cells treated with or without 200 nM doxorubicin for 20 h were labeled with 0.1 μCi/ml [^{3}H]palmitate for additional 4 h. The amount of radio-labeled palmitate

incorporated into ceramide was measured to determine ceramide synthesis activity. *, $p<0.001$. (**B**) Huh7 cells were treated with indicated concentration of myriocin for 2 h before they were treated with 200 nM doxorubicin for 24 h and analyzed as described in Fig. 1B. Similar result was observed in another independent experiment. (**C)** Huh7 cells were treated with or without 30 μM myriocin for 2 h before they were treated with doxorubicin and analyzed as described in Fig. 2C. (**D**) Huh7 cells were treated with indicated concentration of C_6-ceramide for 24 h and analyzed with immunoblot analysis as described in Fig. 1B. Similar result was observed in another independent experiment. (**E**) Indicated cells were treated with indicated concentration of C_6-ceramide for 48 h and analyzed as described in Fig. 2C. (**A, C** and **E)** Results are reported as mean ± S.E.M. of three independent experiments.

Chapter 4: Conclusions and Future Directions

Conclusions and Future Directions

The results of this work demonstrate the importance of CREB3L1 in viral infections and cancer therapy with potential implications in fibrosis. In this section, I will discuss the potential importance of these results as they relate to each scenario as well as future directions to further explore these finding.

The role of CREB3L1 in viral infection

Activation of CREB3L1 through viral infection leads to an up-regulation of genes that prevent progression of the cell cycle as well as an up-regulation of genes responsible for the production of type I collagen. Prevention of cell division in virally infected cells is important for two reasons. For viruses such as HCV that require cell division in order to replicate, the prevention of cell cycle progression stops the virus from creating new viral genomes. Moreover, prevention of cell division avoids one infected cell from becoming multiple infected cells. This point is important for all viral infections as activation of CREB3L1 may play an important role by preventing spread of virus-infected cells. This work demonstrates that the loss of CREB3L1 expression is beneficial to viral propagation.

The role of type I collagen production in viral infection remains unclear, but I propose one possible explanation. Perhaps collagen production somehow creates a barrier around the infected cell and prevents the virus from releasing into circulation. Other

proteins such as BST2/tetherin are known to prevent viral spread by physically restraining virus from escaping which provides some precedent for the idea (Neil et al., 2008). In the case of late stage HCV patients, chronic deposition of collagen may be responsible for the viral infection-induced massive fibrosis that leads to liver failure. To date, the development of fibrosis is very poorly understood. CREB3L1 could be the first step towards understanding fibrosis thus leading to potential treatment.

In regards to targeting CREB3L1 in treating HCV infection, either activation or inhibition of CREB3L1 could be beneficial depending upon the situation. In a newly infected HCV patient, HCV has not selected for cells that lack CREB3L1. In this case, activation of CREB3L1 could prevent HCV from replicating and prevent proliferation of currently infected cells. Ideally, this would lead to clearance of the virus. For late stage HCV patients, fibrosis and subsequent liver failure poses more of a threat than the infection, therefore deactivation of CREB3L1 to prevent collagen deposition could be beneficial for patient survival.

Human Papaloma Virus (HPV) is a human virus that infects epithelial stem cells in the basal stratum of the skin. In order to replenish the epithelium, the stem cells normally undergo epithelial differentiation and divide to form new epithelial layers. HPV infects the epithelial stem cells, but does not replicate in the stem cells. Only after differentiation and cell division does HPV replicate and create new virions (Whiteside et al., 2008). Importantly, HPV replication depends upon progression of the cell cycle of the infected cell. As a result, CREB3L1 may have a role in preventing HPV replication through blockage of epithelial stem cell proliferation. If CREB3L1 plays a role in controlling HPV-infection, monoclonal antibody staining of HPV infected tissue could

show nuclear localization of CREB3L1 as compared to surrounding uninfected tissue. Alternatively, HPV may have mechanisms to block the cleavage or expression of CREB3L1 which would encourage a more detailed study of CREB3L1 in HPV infection.

Animal studies involving CREB3L1 are needed to study the *in vivo* function of CREB3L1 as related to viral infection, fibrosis, and cancer. The preferred way to do animal studies is with a genetic knockout mouse; however, the existing genetic knockout mouse for CREB3L1 has problems with bone development that could hinder these types of studies. Another method is to create a CRE-Lox CREB3L1 mouse that can be crossed with tissue specific CRE-expressing mice to knockout CREB3L1 in a tissue specific manner. For example, lung-specific CREB3L1 knockout mice can be generated for subsequent infection with Sendai virus. This experiment would determine if CREB3L1 lung-specific knockout mice have an increased mortality to Sendai virus infection as compared to wild-type mice.

The role of CREB3L1 in cancer treatment

In clinically relevant concentrations, doxorubicin prevents cancer cells from dividing through activation of CREB3L1 via RIP. Without CREB3L1, doxorubicin cannot exert the anti-proliferative effect. Thus, if cancer cells do not express CREB3L1, doxorubicin will not be a successful treatment. To date, anti-cancer drugs are prescribed because they have worked in the past, not because a diagnostic method exists to determine the effectiveness of the drug. My results could lead to the development of a diagnostic tool that would allow us to tailor doxorubicin therapy or other CREB3L1 - activating drugs only to tumors that express high levels of CREB3L1.

For multiple future directions, a more detailed mechanism of CREB3L1 cleavage by RIP is needed. Currently, we show ceramide triggers transport to the golgi and subsequent cleavage of CREB3L1. One hypothesis is that CREB3L1 can directly sense ceramide in the ER. In this case, CREB3L1 may bind ceramide and trigger the ceramide-CREB3L1 complex to traffic to the golgi. Another possibility is an adaptor protein binds ceramide to regulate CREB3L1 trafficking to the golgi. In this case, the adaptor protein could be a positive or negative regulator of CREB3L1 trafficking. If the adaptor protein positively regulates trafficking, then the ceramide-bound adaptor protein would form a complex with CREB3L1 that would stimulate trafficking of the entire complex to the golgi. If the adaptor protein is a negative regulator, it may draw parallels with regulatory proteins for SREBP2 or ATF6 (Shen et al., 2002; Yang et al., 2002; Yang et al., 2000). If regulated in this fashion, the adaptor protein would normally retain CREB3L1in the ER, but in response to ceramide binding, the adaptor protein would release CREB3L1 for golgi trafficking. In all cases, the results suggest that there is a ceramide sensor in the ER regulates the trafficking of CREB3L1. If an adaptor protein regulates CREB3L1 trafficking, then genetic screening or biochemical pulldown assays may yield the regulating protein.

Another oddity is observed with CREB3L1 RIP in CHO7 cells (Fig. 11). In CHO7 cells, CREB3L1 appears to constitutively traffic to the golgi and is cleaved by S1P yielding a membrane-bound intermediate, but S2P does not cleave unless the cells were treated with doxorubicin. These data suggests another level of regulation for RIP, namely the activation of S2P by doxorubicin, which needs to be explored in the future.

Doxorubicin exerts cardiac toxicity at clinically relevant concentrations demonstrating that it is not extremely specific. The fact that doxorubicin-induced DNA damage occurs in the absence of the anti-proliferative function demonstrates another non-specific effect. Since the mechanism through which doxorubicin blocks proliferation of cancer cells was not known until this body of work, more specific drugs were impossible to screen for or engineer. Although more mechanistic detail is needed, these results set the groundwork for screening of new, more specific drugs that activate CREB3L1 without the side effect toxicities that plague doxorubicin. A chemical library could be screened for drugs that do not affect the growth of MCF7 but do effect the growth of MCF7-CREB3L1(H). Hopefully, this screen would yield new chemotherapy drugs that lack the cardiac toxicities.

Also, drugs that prevent the cleavage of CREB3L1 may prove useful for patients with fibrosis. In this case, one would screen a chemical library co-treated with a drug that induces cleavage such as doxorubicin and look for cells that grow regardless of doxorubicin treatment. Thus, drugs manipulating the CREB3L1 pathway towards either extreme could be very useful for treatment of different diseases.

Appendices

Table 1. Genes with decreased expression in Huh7.5 and HRP-1

Gene	Accession #	Fold Decrease in Huh7.5	Fold Decrease in HRP1
AGR2	AI922323	11.31	73.52
ATP6V0A2	BC022300	21.11	27.86
C4orf18	AF260333	18.38	119.43
CREB3L1	AF055009	11.31	17.15
CTBP2	AF222711	11.31	14.93
FGFR2	M80634	294.07	512.00
GABBR2	AF056085	103.97	27.86
GAD1	NM_013445	13.00	14.93
IGSF9	AB037776	36.76	68.59
ISYNA1	AL137749	11.31	32.00
LBP	M35533	34.30	1260.69
LGALS1	NM_002305	119.43	222.86
LIF	NM_002309	17.15	26.00
LOC284244	AF070541	48.50	39.40
MUC12	AF147790	42.22	48.50
NAT2	NM_000015	39.40	48.50
NNMT	NM_006169	36.76	14.93
OTC	NM_000531	32.00	84.44
PAK7	AB040812	16.00	445.72
PCDHA1-13	AF152308	34.30	119.43
PLAC8	NM_016619	13.93	13.93
PLCL2	AK023546	39.40	168.90
RBP2	NM_004164	13.00	168.90
SEZ6L2	NM_012410	13.00	12.13
SLC2A2	NM_000340	55.72	194.01
TMSL8	NM_021992	21.11	21.11

Table 2. Target genes upregulated by CREB3L1(Δ381-519)

A: Genes encoding inhibitors of the cell cycle

Gene	Accession	Fold Increase
C13orf15 (RGC32)	NM_014059	137.19
EMP1	NM_001423	34.30
SPARC	NM_003118	18.38
PRDM6	AF272898	14.93
CDKN1A (p21)	NM_000389	12.13
PIAS3	NM_006099	8.00
MXI1	NM_005962	8.00
NR4A2	NM_006186	7.46
GADD45γ	NM_006705	6.96
CDKN2C (p18)	NM_001262	5.28

B: Genes involved in type I collagen synthesis

Gene	Accession	Fold Increase
C13orf15 (RGC32)	NM_014059	137.19
COL1A1	BE221212	128.00
COL1A2	NM_000089	42.22
LOX	L16895	25.99
DSE	NM_013352	19.70
SPARC	NM_003118	18.38

C: Other genes

Gene	Accession	Fold Increase
NR4A3	U12767	168.90
CDA	NM_001785	59.71
CYP27B1	NM_000785	25.99
SGMS2	D31421	22.63
CTBP2	BC002486	13.00
FLJ22167	AA401703	12.13
GHR	NM_000163	12.13
SNAP25	NM_003081	12.13
KCNH2	AB044806	12.13
FUT4	AF305083	10.56
IRX5	U90304	10.56

GPSM1	AI242661	9.85
MOBKL2C	BG167841	9.85
PDE4DIP	NM_022359	9.85
HOXA5	NM_019102	9.19
PPM1K	AV706522	9.19
TMEM45A	NM_018004	9.19
NCRNA00153	NM_018474	8.00
ADORA2B	NM_000676	8.00
GAL	AL556409	8.00
PAP2D	AF131783	8.00
CTH	AL354872	8.00
FOSB	NM_006732	8.00
AVPI1	NM_021732	7.46
C2orf88	BE645119	7.46
NPTX2	U26662	6.96
UAP1	S73498	6.96
ASS1	NM_000050	6.50
IGDCC4	AB046848	6.50
TESK2	NM_007170	6.50
TCEAL3	AA847654	6.50
INHBB	NM_002193	6.50
EAF2	NM_018456	6.50
RNF24	NM_007219	6.06
CD55	NM_000574	6.06
ANG	NM_001145	6.06
INHBE	BC005161	6.06
STC2	BC000658	5.66
ST3GAL1	AV721528	5.66
DNAJC6	AV729634	5.66
ICAM3	NM_002162	5.66
FZD9	NM_003508	5.66
TRHDE	NM_013381	5.66
LPPR2	NM_022737	5.66
PAX6	NM_000280	5.66
SNAI1	NM_005985	5.28
ZNF275	BF793625	5.28
HSPA2	U56725	5.28

EPOR	M60459	5.28
RNASE4	NM_002937	5.28
FAM174B	AI801973	5.28

BIBLIOGRAPHY

Adams, C.M., Reitz, J., De Brabander, J.K., Feramisco, J.D., Li, L., Brown, M.S., and Goldstein, J.L. (2004). Cholesterol and 25-hydroxycholesterol inhibit activation of SREBPs by different mechanisms, both involving SCAP and Insigs. J Biol Chem *279*, 52772-52780.

Aman, W., Mousa, S., Shiha, G., and Mousa, S.A. (2012). Current status and future directions in the management of chronic hepatitis C. Virol J *9*, 57.

Appel, N., Schaller, T., Penin, F., and Bartenschlager, R. (2006). From structure to function: new insights into hepatitis C virus RNA replication. J Biol Chem *281*, 9833-9836.

Binder, M., Kochs, G., Bartenschlager, R., and Lohmann, V. (2007). Hepatitis C virus escape from the interferon regulatory factor 3 pathway by a passive and active evasion strategy. Hepatology *46*, 1365-1374.

Blight, K.J., McKeating, J.A., and Rice, C.M. (2002). Highly permissive cell lines for subgenomic and genomic hepatitis C virus RNA replication. J Virol *76*, 13001-13014.

Bose, R., Verheij, M., Haimovitz-Friedman, A., Scotto, K., Fuks, Z., and Kolesnick, R. (1995). Ceramide synthase mediates daunorubicin-induced apoptosis: an alternative mechanism for generating death signals. Cell *82*, 405-414.

Bradshaw, A.D., and Sage, E.H. (2001). SPARC, a matricellular protein that functions in cellular differentiation and tissue response to injury. J Clin Invest *107*, 1049-1054.

Brown, M.S., Ye, J., Rawson, R.B., and Goldstein, J.L. (2000). Regulated intramembrane proteolysis: a control mechanism conserved from bacteria to humans. Cell *100*, 391-398.

Cai, Z., Zhang, C., Chang, K.S., Jiang, J., Ahn, B.C., Wakita, T., Liang, T.J., and Luo, G. (2005). Robust production of infectious hepatitis C virus (HCV) from stably HCV cDNA-transfected human hepatoma cells. J Virol *79*, 13963-13973.

Debelenko, L.V., McGregor, L.M., Shivakumar, B.R., Dorfman, H.D., and Raimondi, S.C. (2011). A novel EWSR1-CREB3L1 fusion transcript in a case of small cell osteosarcoma. Genes Chromosomes Cancer *50*, 1054-1062.

DeBose-Boyd, R.A., Brown, M.S., Li, W.P., Nohturfft, A., Goldstein, J.L., and Espenshade, P.J. (1999). Transport-dependent proteolysis of SREBP: relocation of site-1 protease from Golgi to ER obviates the need for SREBP transport to Golgi. Cell *99*, 703-712

Denard, B., Seemann, J., Chen, Q., Gay, A., Huang, H., Chen, Y., and Ye, J. (2011). The Membrane-Bound Transcription Factor CREB3L1 Is Activated in Response to Virus Infection to Inhibit Proliferation of Virus-Infected Cells. Cell Host Microbe *10*, 65-74.

Dong, X., Feng, H., Sun, Q., Li, H., Wu, T.T., Sun, R., Tibbetts, S.A., Chen, Z.J., and Feng, P. (2010). Murine gamma-herpesvirus 68 hijacks MAVS and IKKbeta to initiate lytic replication. PLoS Pathog *6*, e1001001.

Fox, R.M., Hanlon, C.D., and Andrew, D.J. (2010). The CrebA/Creb3-like transcription factors are major and direct regulators of secretory capacity. J Cell Biol *191*, 479-492.

Gewirtz, D.A. (1999). A critical evaluation of the mechanisms of action proposed for the antitumor effects of the anthracycline antibiotics adriamycin and daunorubicin. Biochem Pharmacol *57*, 727-741.

He, B. (2006). Viruses, endoplasmic reticulum stress, and interferon responses. Cell Death Differ *13*, 393-403.

Honma, Y., Kanazawa, K., Mori, T., Tanno, Y., Tojo, M., Kiyosawa, H., Takeda, J., Nikaido, T., Tsukamoto, T., Yokoya, S., *et al.* (1999). Identification of a novel gene, OASIS, which encodes for a putative CREB/ATF family transcription factor in the long-term cultured astrocytes and gliotic tissue. Brain Res Mol Brain Res *69*, 93-103.

Horton, J.D., Shah, N.A., Warrington, J.A., Anderson, N.N., Park, S.W., Brown, M.S., and Goldstein, J.L. (2003). Combined analysis of oligonucleotide microarray data from transgenic and knockout mice identifies direct SREBP target genes. Proc Natl Acad Sci U S A *100*, 12027-12032.

Hua, X., Sakai, J., Brown, M.S., and Goldstein, J.L. (1996). Regulated cleavage of sterol regulatory element binding proteins requires sequences on both sides of the endoplasmic reticulum membrane. J Biol Chem *271*, 10379-10384.

Huang, H., Sun, F., Owen, D.M., Li, W., Chen, Y., Gale, M., Jr., and Ye, J. (2007). Hepatitis C virus production by human hepatocytes dependent on assembly and secretion of very low-density lipoproteins. Proc Natl Acad Sci U S A *104*, 5848-5853.

Hurlin, P.J., and Huang, J. (2006). The MAX-interacting transcription factor network. Semin Cancer Biol *16*, 265-274.

Kondo, S., Murakami, T., Tatsumi, K., Ogata, M., Kanemoto, S., Otori, K., Iseki, K., Wanaka, A., and Imaizumi, K. (2005). OASIS, a CREB/ATF-family member, modulates UPR signalling in astrocytes. Nat Cell Biol *7*, 186-194.

Lee, V.W., and Harris, D.C. (2011). Adriamycin nephropathy: a model of focal segmental glomerulosclerosis. Nephrology (Carlton) *16*, 30-38.

Liang, G., Yang, J., Horton, J.D., Hammer, R.E., Goldstein, J.L., and Brown, M.S. (2002). Diminished hepatic response to fasting/refeeding and liver X receptor agonists in mice with selective deficiency of sterol regulatory element-binding protein-1c. J Biol Chem *277*, 9520-9528.

Liebermann, D.A., and Hoffman, B. (2002). Myeloid differentiation (MyD)/growth arrest DNA damage (GADD) genes in tumor suppression, immunity and inflammation. Leukemia *16*, 527-541.

Lohmann, V., Korner, F., Koch, J., Herian, U., Theilmann, L., and Bartenschlager, R. (1999). Replication of subgenomic hepatitis C virus RNAs in a hepatoma cell line. Science *285*, 110-113.

Martinon, F., and Glimcher, L.H. (2011). Regulation of innate immunity by signaling pathways emerging from the endoplasmic reticulum. Curr Opin Immunol *23*, 35-40.

Medigeshi, G.R., Lancaster, A.M., Hirsch, A.J., Briese, T., Lipkin, W.I., Defilippis, V., Fruh, K., Mason, P.W., Nikolich-Zugich, J., and Nelson, J.A. (2007). West Nile virus infection activates the unfolded protein response, leading to CHOP induction and apoptosis. J Virol *81*, 10849-10860.

Mertens, F., Fletcher, C.D., Antonescu, C.R., Coindre, J.M., Colecchia, M., Domanski, H.A., Downs-Kelly, E., Fisher, C., Goldblum, J.R., Guillou, L., *et al.* (2005). Clinicopathologic and molecular genetic characterization of low-grade fibromyxoid sarcoma, and cloning of a novel FUS/CREB3L1 fusion gene. Lab Invest *85*, 408-415.

Metherall, J.E., Goldstein, J.L., Luskey, K.L., and Brown, M.S. (1989). Loss of transcriptional repression of three sterol-regulated genes in mutant hamster cells. J Biol Chem *264*, 15634-15641.

Miyake, Y., Kozutsumi, Y., Nakamura, S., Fujita, T., and Kawasaki, T. (1995). Serine palmitoyltransferase is the primary target of a sphingosine-like immunosuppressant, ISP-1/myriocin. Biochem Biophys Res Commun *211*, 396-403.

Moller, E., Hornick, J.L., Magnusson, L., Veerla, S., Domanski, H.A., and Mertens, F. (2011). FUS-CREB3L2/L1-positive sarcomas show a specific gene expression profile with upregulation of CD24 and FOXL1. Clin Cancer Res *17*, 2646-2656.

Moradpour, D., Penin, F., and Rice, C.M. (2007). Replication of hepatitis C virus. Nat Rev Microbiol *5*, 453-463.

Murakami, T., Kondo, S., Ogata, M., Kanemoto, S., Saito, A., Wanaka, A., and Imaizumi, K. (2006). Cleavage of the membrane-bound transcription factor OASIS in response to endoplasmic reticulum stress. J Neurochem *96*, 1090-1100.

Murakami, T., Saito, A., Hino, S., Kondo, S., Kanemoto, S., Chihara, K., Sekiya, H., Tsumagari, K., Ochiai, K., Yoshinaga, K., *et al.* (2009). Signalling mediated by the endoplasmic reticulum stress transducer OASIS is involved in bone formation. Nat Cell Biol *11*, 1205-1211.

Nakabayashi, H., Taketa, K., Miyano, K., Yamane, T., and Sato, J. (1982). Growth of human hepatoma cells lines with differentiated functions in chemically defined medium. Cancer Res *42*, 3858-3863.

Neil, S.J., Zang, T., and Bieniasz, P.D. (2008). Tetherin inhibits retrovirus release and is antagonized by HIV-1 Vpu. Nature *451*, 425-430.

Nikaido, T., Yokoya, S., Mori, T., Hagino, S., Iseki, K., Zhang, Y., Takeuchi, M., Takaki, H., Kikuchi, S., and Wanaka, A. (2001). Expression of the novel transcription factor OASIS, which belongs to the CREB/ATF family, in mouse embryo with special reference to bone development. Histochem Cell Biol *116*, 141-148.

Pietschmann, T., Lohmann, V., Rutter, G., Kurpanek, K., and Bartenschlager, R. (2001). Characterization of cell lines carrying self-replicating hepatitis C virus RNAs. J Virol *75*, 1252-1264.

Rawson, R.B., Cheng, D., Brown, M.S., and Goldstein, J.L. (1998). Isolation of cholesterol-requiring mutant Chinese hamster ovary cells with defects in cleavage of sterol regulatory element-binding proteins at site 1. J Biol Chem *273*, 28261-28269.

Rawson, R.B., Zelenski, N.G., Nijhawan, D., Ye, J., Sakai, J., Hasan, M.T., Chang, T.Y., Brown, M.S., and Goldstein, J.L. (1997). Complementation cloning of S2P, a gene encoding a putative metalloprotease required for intramembrane cleavage of SREBPs. Mol Cell *1*, 47-57.

Rice, C.M. (2011). New insights into HCV replication: potential antiviral targets. Topics in antiviral medicine *19*, 117-120.

Saigusa, K., Imoto, I., Tanikawa, C., Aoyagi, M., Ohno, K., Nakamura, Y., and Inazawa, J. (2007). RGC32, a novel p53-inducible gene, is located on centrosomes during mitosis and results in G2/M arrest. Oncogene *26*, 1110-1121.

Sakai, J., Duncan, E.A., Rawson, R.B., Hua, X., Brown, M.S., and Goldstein, J.L. (1996). Sterol-regulated release of SREBP-2 from cell membranes requires two sequential cleavages, one within a transmembrane segment. Cell *85*, 1037-1046.

Scholle, F., Li, K., Bodola, F., Ikeda, M., Luxon, B.A., and Lemon, S.M. (2004). Virus-host cell interactions during hepatitis C virus RNA replication: impact of polyprotein expression on the cellular transcriptome and cell cycle association with viral RNA synthesis. J Virol *78*, 1513-1524.

Shen, J., Chen, X., Hendershot, L., and Prywes, R. (2002). ER stress regulation of ATF6 localization by dissociation of BiP/GRP78 binding and unmasking of Golgi localization signals. Dev Cell *3*, 99-111.

Sherr, C.J., and Roberts, J.M. (1999). CDK inhibitors: positive and negative regulators of G1-phase progression. Genes Dev *13*, 1501-1512.

Soule, H.D., Vazguez, J., Long, A., Albert, S., and Brennan, M. (1973). A human cell line from a pleural effusion derived from a breast carcinoma. J Natl Cancer Inst *51*, 1409-1416.

Stahelin, H.F., and von Wartburg, A. (1991). The chemical and biological route from podophyllotoxin glucoside to etoposide: ninth Cain memorial Award lecture. Cancer Res *51*, 5-15.

Sumpter, R., Jr., Loo, Y.M., Foy, E., Li, K., Yoneyama, M., Fujita, T., Lemon, S.M., and Gale, M., Jr. (2005). Regulating intracellular antiviral defense and permissiveness to hepatitis C virus RNA replication through a cellular RNA helicase, RIG-I. J Virol *79*, 2689-2699.

Sumpter, R., Jr., Wang, C., Foy, E., Loo, Y.M., and Gale, M., Jr. (2004). Viral evolution and interferon resistance of hepatitis C virus RNA replication in a cell culture model. J Virol *78*, 11591-11604.

Tardif, K.D., Mori, K., and Siddiqui, A. (2002). Hepatitis C virus subgenomic replicons induce endoplasmic reticulum stress activating an intracellular signaling pathway. J Virol *76*, 7453-7459.

Thompson, A.J., Locarnini, S.A., and Beard, M.R. (2011). Resistance to anti-HCV protease inhibitors. Current opinion in virology *1*, 599-606.

Tse, M.T. (2010). New oral HCV drug shows promise. Nat Rev Microbiol *8*, 464.

van Marle, G., Antony, J., Ostermann, H., Dunham, C., Hunt, T., Halliday, W., Maingat, F., Urbanowski, M.D., Hobman, T., Peeling, J., *et al.* (2007). West Nile virus-induced neuroinflammation: glial infection and capsid protein-mediated neurovirulence. J Virol *81*, 10933-10949.

Vellanki, R.N., Zhang, L., Guney, M.A., Rocheleau, J.V., Gannon, M., and Volchuk, A. (2010). OASIS/CREB3L1 induces expression of genes involved in extracellular matrix

production but not classical endoplasmic reticulum stress response genes in pancreatic beta-cells. Endocrinology *151*, 4146-4157.

von dem Bussche, A., Machida, R., Li, K., Loevinsohn, G., Khander, A., Wang, J., Wakita, T., Wands, J.R., and Li, J. (2010). Hepatitis C virus NS2 protein triggers endoplasmic reticulum stress and suppresses its own viral replication. J Hepatol *53*, 797-804.

Vrolijk, J.M., Kaul, A., Hansen, B.E., Lohmann, V., Haagmans, B.L., Schalm, S.W., and Bartenschlager, R. (2003). A replicon-based bioassay for the measurement of interferons in patients with chronic hepatitis C. J Virol Methods *110*, 201-209.

Wakita, T., Pietschmann, T., Kato, T., Date, T., Miyamoto, M., Zhao, Z., Murthy, K., Habermann, A., Krausslich, H.G., Mizokami, M., *et al.* (2005). Production of infectious hepatitis C virus in tissue culture from a cloned viral genome. Nat Med *11*, 791-796.

Wang, C., Gale, M., Jr., Keller, B.C., Huang, H., Brown, M.S., Goldstein, J.L., and Ye, J. (2005). Identification of FBL2 as a geranylgeranylated cellular protein required for hepatitis C virus RNA replication. Mol Cell *18*, 425-434.

Whiteside, M.A., Siegel, E.M., and Unger, E.R. (2008). Human papillomavirus and molecular considerations for cancer risk. Cancer *113*, 2981-2994.

Yamamoto, T., Davis, C.G., Brown, M.S., Schneider, W.J., Casey, M.L., Goldstein, J.L., and Russell, D.W. (1984). The human LDL receptor: a cysteine-rich protein with multiple Alu sequences in its mRNA. Cell *39*, 27-38.

Yang, T., Espenshade, P.J., Wright, M.E., Yabe, D., Gong, Y., Aebersold, R., Goldstein, J.L., and Brown, M.S. (2002). Crucial step in cholesterol homeostasis: sterols promote binding of SCAP to INSIG-1, a membrane protein that facilitates retention of SREBPs in ER. Cell *110*, 489-500.

Yang, T., Goldstein, J.L., and Brown, M.S. (2000). Overexpression of membrane domain of SCAP prevents sterols from inhibiting SCAP.SREBP exit from endoplasmic reticulum. J Biol Chem *275*, 29881-29886.

Ye, J. (2007). Reliance of host cholesterol metabolic pathways for the life cycle of hepatitis C virus. PLoS Pathog *3*, e108.

Ye, J., Dave, U.P., Grishin, N.V., Goldstein, J.L., and Brown, M.S. (2000a). Asparagine-proline sequence within membrane-spanning segment of SREBP triggers intramembrane cleavage by site-2 protease. Proc Natl Acad Sci U S A *97*, 5123-5128.

Ye, J., Rawson, R.B., Komuro, R., Chen, X., Dave, U.P., Prywes, R., Brown, M.S., and Goldstein, J.L. (2000b). ER stress induces cleavage of membrane-bound ATF6 by the same proteases that process SREBPs. Mol Cell *6*, 1355-1364.

Ye, J., Wang, C., Sumpter, R., Jr., Brown, M.S., Goldstein, J.L., and Gale, M., Jr. (2003). Disruption of hepatitis C virus RNA replication through inhibition of host protein geranylgeranylation. Proc Natl Acad Sci U S A *100*, 15865-15870.

Yuan, H.J., Jain, M., Snow, K.K., Gale, M., Jr., and Lee, W.M. (2010). Evolution of hepatitis C virus NS5A region in breakthrough patients during pegylated interferon and ribavirin therapy*. J Viral Hepat *17*, 208-216.

Zein, N.N. (2000). Clinical significance of hepatitis C virus genotypes. Clin Microbiol Rev *13*, 223-235.